(12) INTERNATIONAL APPLICATION PUBLISHED UNDER THE PATENT COOPERATION TREATY (PCT)

(19) World Intellectual Property Organization
International Bureau

(43) International Publication Date
15 November 2012 (15.11.2012)

WIPO | PCT

(10) International Publication Number
WO 2012/155055 A2

(51) International Patent Classification:
A61K 49/06 (2006.01) *A61K 39/395* (2006.01)
A61K 49/04 (2006.01) *A61P 9/00* (2006.01)
A61K 47/48 (2006.01) *A61P 29/00* (2006.01)

(21) International Application Number:
PCT/US2012/037546

(22) International Filing Date:
11 May 2012 (11.05.2012)

(25) Filing Language: English

(26) Publication Language: English

(30) Priority Data:
61/484,892 11 May 2011 (11.05.2011) US

(71) Applicant *(for all designated States except US)*: **YALE UNIVERSITY** [US/US]; Two Whitney Avenue, New Haven, CT 06511 (US).

(72) Inventors; and
(75) Inventors/Applicants *(for US only)*: **SADEGHI, Mehran, M.** [CA/US]; 340 Falls Road, Bethany, CT 06524 (US). **SINUSAS, Albert, J.** [US/US]; 490 Briarwood Drive, Guilford, CT 06437 (US).

(74) Agent: **COLEMAN, Henry, D.**; Coleman Sudol Sapone, P.C., 714 Colorado Avenue, Bridgeport, CT 06605-1601 (US).

(81) Designated States *(unless otherwise indicated, for every kind of national protection available)*: AE, AG, AL, AM, AO, AT, AU, AZ, BA, BB, BG, BH, BR, BW, BY, BZ, CA, CH, CL, CN, CO, CR, CU, CZ, DE, DK, DM, DO, DZ, EC, EE, EG, ES, FI, GB, GD, GE, GH, GM, GT, HN, HR, HU, ID, IL, IN, IS, JP, KE, KG, KM, KN, KP, KR, KZ, LA, LC, LK, LR, LS, LT, LU, LY, MA, MD, ME, MG, MK, MN, MW, MX, MY, MZ, NA, NG, NI, NO, NZ, OM, PE, PG, PH, PL, PT, QA, RO, RS, RU, RW, SC, SD, SE, SG, SK, SL, SM, ST, SV, SY, TH, TJ, TM, TN, TR, TT, TZ, UA, UG, US, UZ, VC, VN, ZA, ZM, ZW.

(84) Designated States *(unless otherwise indicated, for every kind of regional protection available)*: ARIPO (BW, GH, GM, KE, LR, LS, MW, MZ, NA, RW, SD, SL, SZ, TZ, UG, ZM, ZW), Eurasian (AM, AZ, BY, KG, KZ, RU, TJ, TM), European (AL, AT, BE, BG, CH, CY, CZ, DE, DK, EE, ES, FI, FR, GB, GR, HR, HU, IE, IS, IT, LT, LU, LV, MC, MK, MT, NL, NO, PL, PT, RO, RS, SE, SI, SK, SM, TR), OAPI (BF, BJ, CF, CG, CI, CM, GA, GN, GQ, GW, ML, MR, NE, SN, TD, TG).

Published:

— *without international search report and to be republished upon receipt of that report (Rule 48.2(g))*

WO 2012/155055 A2

(54) Title: INTEGRIN-TARGETED IMAGING OF INFLAMMATION IN VASCULAR REMODELING

(57) Abstract: The invention provides methods of assessing in real time the likelihood that a subject suffers from, or is risk of developing, a vascular disorder, the method comprising: (a) arterially administering a detectable ligand having a binding affinity for $\alpha v\beta 3$ integrin to the subject, measuring the subject's vascular uptake of the detectable ligand, and comparing the subject's vascular uptake of the detectable ligand to a standard or control, wherein an increase in the subject's vascular uptake of the detectable ligand when compared to the standard or control sample indicates that the subject suffers from, or is risk of developing, a vascular disease; and optionally (b) imaging the subject's vascular walls to assess vascular wall remodeling. The invention also provides methods of assessing in real time the efficacy of vascular disorder treatments.

Integrin-Targeted Imaging of Inflammation in Vascular Remodeling

Related Applications and Government Support

This application claims priority from U.S. Provisional Application Serial No. 61/484,892, filed May 11, 2011, the complete disclosure of which is hereby incorporated by reference in their entirety.

The invention described herein was funded in part by NIH Grant Nos. R01HL085093 and P01HL70295 and a Department of Veterans Affairs Merit Grant. Accordingly, the United States has certain rights in the invention.

Background of the Invention

Inflammation is a common feature of many vascular diseases and plays a central role in their pathogenesis. Typical examples include atherosclerosis and aneurysm formation where an inflammatory process is critical to the development of the disease and its complications. It is therefore not surprising that many therapeutic interventions aim at modulating vessel wall inflammation. One of the limitations of the modern approach to managing vascular diseases is the lack of reliable approaches to detecting, and tracking the effect of interventions on, vessel wall biology. This may be addressed by targeting molecular signatures of relevant process by molecular imaging.

Endothelial activation, leukocyte recruitment and activation, and matrix remodeling are integral parts of inflammation, which is closely intertwined with vessel wall angiogenesis. αv integrin-targeted imaging has been introduced for detecting angiogenesis associated with myocardial infarction [1], peripheral arterial disease [2], atherosclerosis [3] and neoplasm [4]. This led us to investigate whether α_v-targeted imaging may be used for detection of vessel wall inflammation *in vivo*.

Integrins are a large family of heterodimeric adhesion molecules which mediate cell-cell and cell-matrix interactions 13. In vertebrates, 8 β subunits associate with 18 α subunits to generate 24 distinct integrins. Most integrins bind to ligands which contain an RGD tripeptide sequence. An important aspect of integrin biology is the role of conformational

changes which modulate integrin function. Many integrins are expressed in a low affinity (off) state and upon activation, whether through outside-in or inside-out signals, convert to a high affinity (on) state which can bind specific ligands and trigger signaling [13]. Integrin activation state is cell-dependent. For example, $\alpha_v\beta_3$ integrin is mostly in a low affinity state in JY lymphoblastoid cells, while in melanoma cell lines it is present in an active conformation [14]. In resting ECs, $\alpha_v\beta_3$ is mostly in a low affinity state and EC activation, e.g., with shear stress, increases high affinity integrin [12].

Integrin $\alpha_v\beta_3$ is expressed at high density on proliferating ECs and $\alpha_v\beta_3$-targeted imaging appears as a promising approach for detection of angiogenesis associated with tumors a and myocardial or hindlimb ischemia [1, 2]. Expression of $\alpha_v\beta_3$ integrins by other cells raises the possibility that this integrin may be targeted for imaging other processes where cell proliferation and integrin-mediated cell-cell and cell-matrix interactions are critically involved. Indeed, RP748, an ^{111}In-labeled $\alpha_v\beta_3$-targeted tracer localizes in murine or human arteries following mechanical or immune injury in parallel with changes in cell proliferation. [7, 11].

Several tracers have been developed for imaging $\alpha_v\beta_3$expression, predominantly in angiogenesis [17-19]. In general, the binding motif in these probes is structured based on RGD tripeptide and they show broader specificity for α_v integrins. We have previously shown that RP748, a peptidomimetic quinolone, preferentially interacts with the active conformation of the integrin 1r.

Summary of the Invention

The present invention relates to the discovery that α_v-targeted imaging methods may be used for detection of vessel wall inflammation *in vivo,* enabling prompt diagnoses and treatment of a wide variety of vascular diseases.

Accordingly, in one embodiment, the present invention provides a method of assessing a vascular disease as defined hereinafter, and optionally, vascular remodeling in said subject, the method comprising:

(a) administering (preferably, intravenously) a detectable ligand (i.e., detectable using single photon emission tomography (SPECT), positron emission tomography (PET), near-infrared (NIR) fluorescence (e.g. around 700–1,000 nm) detection, magnetic resonance imaging

(MRI), optical imaging and/or optoacoustic imaging) having a binding affinity for integrin (preferably $\alpha_v\beta_3$ activated integrin) to the subject, measuring the subject's vascular uptake (through integrin binding, preferably activated integrin binding) of the detectable ligand, and comparing the subject's vascular uptake of the detectable ligand to a first standard or control, wherein an increase in the subject's vascular uptake of the detectable ligand when compared to the standard or control indicates that the subject suffers from, or is risk of developing, a vascular disease or its complications; and optionally

(b) imaging the subject's vascular walls to assess vascular wall remodeling as defined hereinafter, e.g. using single photon emission tomography (SPECT), positron emission tomography (PET), near-infrared (NIR) fluorescence (e.g. around 700–1,000 nm) detection, magnetic resonance imaging (MRI), ultrasound, optical imaging and/or optoacoustic imaging, wherein the presence of vascular wall remodeling when compared to a second standard or control indicates that the subject suffers from, or is risk of developing, a vascular disease.

The above method may be used to assess the likelihood that a subject suffers from, or is at risk of developing a vascular disease as otherwise described herein (often an aortic aneurysm, atherosclerosis, the occurrence of adverse vascular events (acute coronary syndromes & stroke), vasculitis and transplant vasculopathy, assessing or tracking the effect of therapeutic intervention on vascular disease, as well as assessing vascular wall remodeling, including the likelihood that vascular wall remodeling will occur or will worsen.

In embodiments of the invention, the above method is often used to detect aortic aneurysm, wherein the uptake is linked to aortic aneurysm expansion and patient stratification based upon the risk of rupture (control values may be provided for these). In additional preferred embodiments, the above method may be used to track therapeutic interventions, as well as assess the risk of endoleak after stent placement. The above method is also useful in assessing atherosclerosis, particularly detection of inflammatory components as a way to assess plaque vulnerability and risk of adverse vascular events (e.g. acute coronary syndromes & stroke), as well as tracking the effect of therapeutic intervention in atherosclerosis. The above method is also often used for diagnosis and tracking the effect of therapeutic interventions in vasculitis. It is noted that in certain embodiments the present invention focuses on inflammatory components which are associated with activated integrins which bind to ligands which assist in measuring these activated integrins. From the

measurement of the activated integrins, a diagnosis, prognosis and/or prediction as otherwise described herein may be made, especially including for aortic aneurysym.

In further embodiments of the present invention, the detectable ligand is often a radiolabeled RGD peptide selected from the group consisting of ^{99m}Tc-NC100692, ^{18}F-AH585, ^{111}IN-RP748 , ^{18}F-galacto-RGD and ^{99m}Tc-3PRGD2, more often ^{99m}Tc-NC100692 and ^{18}F-AH585, even more often ^{99m}Tc-NC100692. In preferred aspects of the invention, the inventive method focuses on uptake of the detectable ligand (e.g., a labeled peptide as presented above) by activated integrins. In alternative aspects, the invention focuses on imaging inflammatory processes (especially atheroslerosis). In still other aspects of the invention, the method focuses on assessing aortic aneurysm, vasculitis and transplant vasculopathy (chronic allograft rejection). The use of ^{99m}Tc-NC100692 may be preferred because NC100692 as a ligand (as well as certain other RGD peptide ligands) exhibits preferred binding for activated integrin (a higher affinity state which occurs as a consequence of a conformational change in the in the vascular wall) and provides exceptionally accurate data related to inflammation of the vascular wall which is useful in the present invention.

Alternatively, in one embodiment, the present invention provides a method of assessing vascular remodeling and consequently, the likelihood that a subject suffers from, or is at risk of developing, a vascular disease as defined hereinafter, the method comprising:
(a) administering (preferably, intravenously) a ligand detectable using single photon emission tomography (SPECT), positron emission tomography (PET), near-infrared (NIR) fluorescence (e.g. around 700–1,000 nm) detection, magnetic resonance imaging (MRI), ultrasound, optical imaging and/or optoacoustic imaging having a binding affinity for integrin (often $\alpha_v\beta_3$ integrin, especially activated integrin) in the vascular walls of said subject, imaging the subject's vascular walls, and comparing the image of the subject's vascular walls to a first standard or control, wherein an increase in the subject's vascular uptake of the detectable ligand when compared to the standard or control indicates the presence of vascular remodeling in said subject, or the risk of vascular remodeling or further vascular remodeling in said subject; and optionally
(b) measuring the subject's vascular uptake of the detectable ligand using single photon emission tomography (SPECT), positron emission tomography (PET), near-infrared (NIR) fluorescence (e.g. around 700–1,000 nm) detection, magnetic resonance imaging (MRI), ultrasound, optical imaging and/or optoacoustic imaging, and comparing the subject's

vascular uptake of the detectable ligand to a second standard or control, wherein an increase in the subject's vascular uptake of the detectable ligand when compared to the standard or control indicates that the subject suffers from, or is risk of developing, a vascular disease or its complications.

In preferred aspects of the invention as above, method may be used to assess vascular remodeling in the subject, including the likelihood that vascular wall remodeling will occur or will worsen, and optionally the likelihood that a subject suffers from, or is at risk of developing a vascular disease as otherwise described herein (often an aortic aneurysm, atherosclerosis, the occurrence of vascular events (acute coronary syndromes & stroke), vasculitis and transplant vasculopathy, and/or assessing or tracking the effect of therapeutic intervention on vascular disease in said subject.

As described, the method may be used often to detect aortic aneurysm, to track therapeutic interventions, as well as assess the risk of endoleak after stent placement. The above method is also useful in assessing atherosclerosis, the detection of inflammatory components and adverse vascular events (e.g. acute coronary syndromes & stroke), as well as tracking the effect of therapeutic intervention in atherosclerosis, vasculitis and transplant vasculopathy (chronic allograft rejection), especially by measuring activated integrins to which a ligand is bound.

In further embodiments of the present invention, the detectable ligand is often a radiolabeled RGD peptide selected from the group consisting of ^{99m}Tc-NC100692, ^{18}F-AH111585, ^{111}In-RP748 , ^{18}F-galacto-RGD and ^{99m}Tc-3PRGD2, more often ^{99m}Tc-NC100692 and ^{18}F-AH111585, even more often ^{99m}Tc-NC100692. In preferred aspects of the invention, the inventive method focuses on uptake of the detectable ligand (e.g., a labeled peptide as presented above) by activated integrins. In alternative aspects, the invention focuses on imaging inflammatory processes (especially atherosclerosis), which may be monitored by measuring activated integrin (especially $\alpha_v\beta_3$ integrin) using the methods of the present invention. In still other aspects of the invention, the method focuses on assessing aortic aneurysm, vasculitis and transplant vasculopathy (chronic allograft rejection).

In another embodiment, the invention provides a method of assessing, often in real time, the efficacy of a vascular disease treatment (including the ability to predict vascular

remodeling in response to treatments) which has been administered to a subject who has been diagnosed as suffering from a vascular disease as defined hereinafter, the method comprising: (a) administering (preferably intravenously) a detectable ligand having a binding affinity for $\alpha_v\beta_3$ integrin (in preferred aspects, activated integrin) to the subject, measuring the subject's vascular uptake of the detectable ligand, and comparing the subject's vascular uptake of the detectable ligand to a first standard or control, wherein a decrease in the subject's vascular uptake of the detectable ligand when compared to the standard or control indicates that the treatment is effective in treating the vascular disease; and optionally
(b) imaging the subject's vascular walls to assess and/or predict vascular wall remodeling, e.g. using single photon emission tomography (SPECT), positron emission tomography (PET), or near-infrared (NIR) fluorescence (e.g. around 700–1,000 nm) detection, magnetic resonance imaging (MRI), ultrasound, ultrasound, optical imaging and/or optoacoustic imaging, wherein a decrease in or absence of vascular wall remodeling when compared to a second standard or control indicates that the treatment is effective in treating the vascular disease.

In preferred aspects, the method is directed to assessing the efficacy of treatment of atherosclerosis, vasculitis and/or transplant vasculopathy (chronic allograft rejection), among others.

"Assessing (often in real time) the likelihood that a subject suffers from, or is risk of developing, a vascular disease", or "assessing (often in real time) the efficacy of a vascular disease treatment" can include diagnosing a subject, providing a prognosis for treatment or assessing a treatment efficacy over a period of at least about 60, 50, 45, 40, 35, 30, 25, 20, 15, 14, 13, 12, 11 10, 9, 8, 7, 6, 5, 4, 3, 2, or 1 day, or around 48-36, or around 36-24, or around 24-12, or around 12-6, or around 6-1 hours, or around 60-45, or 45-30, or 30-15, or less than 15 minutes after a subject presents for diagnosis or begins treatment. Assessing the efficacy of a vascular disease treatment often includes the ability to predict vascular remodeling in response to treatment. In one embodiment, the present application is directed to the ability to predict vascular remodeling in response to treatment of vascular disease.

In certain embodiments, the "detectable ligand having a binding affinity for $\alpha_v\beta_3$ integrin" includes but is not limited to labeled NC100692, detectable versions of the antibodies disclosed in United States Patent No. 6,171,588, Vitaxin (humanized antibody

composed of human IgG-1, kappa and the complement domain regions of the murine antibody LM 609), Vitaxin-2–conjugated, gadolinium-encapsulated nanoparticles and other detectable monoclonal $\alpha_v\beta_3$ integrin antibodies, detectable versions of the small molecule $\alpha_v\beta_3$ integrins disclosed in or incorporated by reference in United States Patent No. 7,566,442, and detectable naturally occurring or synthetic peptides and peptidomimetics (generically referred to as "a detectable αvβ3 integrin binding peptide" or alternatively, a "detectable RGD peptide" wherein each of the binding peptides is labeled with a SPECT, PET or NIR reporter), including but not limited to ^{111}In-MSAP-RGD, (^{18})F-galacto-RGD ((^{18})F-RGD, (^{18})F-AlF-NOTA-PRGD2, [(^{99m})Tc]HYNIC-RGD [6-hydrazinonicotinic acid conjugated to cyclo(Arg-Gly-Asp-D-Phe-Lys), (^{99m})Tc-RAFT-RAD, (^{64})Cu-RGD, (^{18})F-galacto-RGD, (^{99m})Tc-RAFT-RAD, ^{18}F-FBEM. [^{18}F]fluciclatide, ^{111}In-labeled 1,4,7,10-tetraazacyclododecane-1,4,7,10-tetracetic acid (DOTA)-Glu{PEG4-Glu[cyclo(Lys(Gly-Gly-Gly)-Arg-Gly-Asp-d-Phe)]-cyclo(Lys(Gly-Gly-Gly)-Arg-Gly-Asp-d-Phe)}-{PEG4-Glu[cyclo(Lys(Gly-Gly-Gly)-Arg-Gly-Asp-d-Phe)]-cyclo(Lys(Gly-Gly-Gly)-Arg-Gly-Asp-d-Phe)}, abbreviated as 111In(DOTA-2P4G-RGD4) or ^{111}In-DOTA-E{PEG4-E[Gly3-c(RGDfK)]2}2, RGD multimers such as those disclosed or referenced in Shan, Molecular Imaging and Contrast Agent Database (MICAD) [Internet] Bethesda (MD): National Center for Biotechnology Information (US); 2004-2011.2012 Feb 23; RGD4C/Cy5.5-ferritin 64Cu-loaded nanocages (RGD4C/Cy5.5-Fn-64Cu nanocages); nanoshell (NS)-RGDfK, cyclic peptide LXW7, and 3-substituted tetrahydro-[1,8]naphthyridine–containing αvβ3 antagonists and other detectable ligands specific for αvβ3 integrin as disclosed or referenced in Shan, Molecular Imaging and Contrast Agent Database (MICAD) [Internet]. Bethesda (MD): National Center for Biotechnology Information (US); 2004-2010. (2010 Jan 06).

NC100692 is also known as "maraciclatide" [D.Edwards *et al*, Nucl.Med.Biol., 35, 365-375 (2008)]. The chemical name is: 1,5-pentanedioic acid-(5-[2-hydroxyimino-1,1-dimethyl-propylamino]-3-(2-[2-hydroxyimido-1,1-dimethyl-propylamino]-ethyl)-pentyl)-amide 5-[13-benzyl-19-carboxymethyl-25-(3-guanidino-propyl)-10-(4,7,10,16-tetraoxa-14,18-dioxo-1,13,19-triazanonadecyl)-carbamoyl-3,6,12,15,18,21,24,27-octaoxo-8,29,30-trithia-2,5,11,14,17,20,23,26-octaaza-bicyclo[14.11.4]hentriacont-4-yl] pentyl-amide. This ligand is often preferred for use in the present invention because of its ability to selectively bind to activated integrin (especially including $\alpha_v\beta_3$ integrin which is activated) and allow accurate quantitation of the binding of that integrin and its relationship to vascular inflammation. The chemical structure of maraciclatide is as follows:

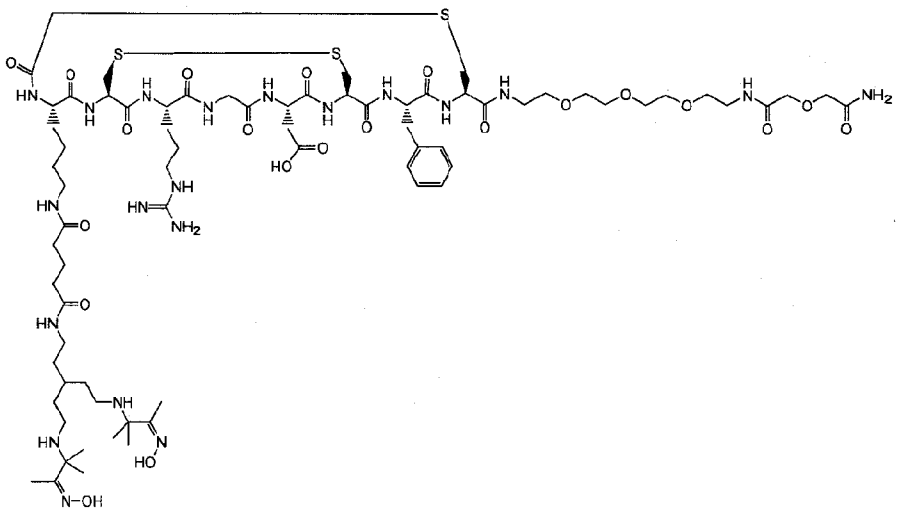

Maraciclatide

In certain embodiments of the invention, the detectable ligand having a binding affinity for $\alpha_v\beta_3$ integrin is comprised of an $\alpha_v\beta_3$ integrin antibody or antibody derivative (including an antibody fragment) which is derivatized with or linked to a detectable moiety which is preferably selected from the group consisting of: (a) a fluorescent label; (b) the bio-luminescent labels luciferase and luciferin; (c) a sensitizer; (d) a coenzyme or enzyme substrate; (e) a radiolabel; (g) labelled avidin or streptavidin; (h) a latex or carbon particle; and (i) biotin, digoxygenin or 5-bromodeoxyuridine.

In a preferred embodiment, the methods of assessing (often in real time) the likelihood that a subject suffers from, or is risk of developing, a vascular disease or its complications, and assessing (often in real time) the efficacy of a vascular disease treatment, including predicting the outcome of therapy, comprise the steps of:

(a) administering (preferably intravenously) a detectable ligand having a binding affinity for $\alpha_v\beta_3$ integrin to the subject, said detectable ligand being selected from the group consisting of ^{111}In-MSAP-RGD, (18)F-galacto-RGD, ((18)F-RGD, (18)F-AlF-NOTA-PRGD2, [(99m)Tc]HYNIC-RGD [6-hydrazinonicotinic acid conjugated to cyclo(Arg-Gly-Asp-D-Phe-Lys), (99m)Tc-RAFT-RAD, (64)Cu-RGD, 18F-FBEM and [18F]fluciclatide;

(b) measuring the subject's vascular uptake of the detectable ligand using single photon emission tomography (SPECT), positron emission tomography (PET), near-infrared (NIR)

fluorescence (e.g. around 700–1,000 nm) detection, magnetic resonance imaging (MRI), ultrasound, optical imaging and/or optoacoustic imaging; and optionally
(c) imaging the subject's vascular walls to assess vascular wall remodeling using single photon emission tomography (SPECT), positron emission tomography (PET), near-infrared (NIR) fluorescence (e.g. around 700–1,000 nm) detection, magnetic resonance imaging (MRI), ultrasound, optical imaging and/or optoacoustic imaging.

Significantly, methods of the invention facilitate rapid diagnosis and treatment of vascular diseases such as ischemic stroke, hemorrhagic stroke, transient ischemic attack (TIA), atherosclerosis, myocardial infarction and arrhythmia, peripheral vascular disease and cerebral vascular disease, and venous occlusive disorders such as deep vein thrombosis, aneurysm (including AAA and TAA), vasculitis and transplant vasculopathy. Further, the methods of the invention provide real-time treatment efficacy information that enables healthcare providers to optimize treatment of such disorders and prevents potentially life-threatening delays in selecting proper treatment modalities.

Inflammation plays a key role in the pathogenesis of several vasculopathies, including atherosclerosis and aneurysm, among other disease states, as set forth herein. In atherosclerosis, vessel wall inflammation has been linked to plaque vulnerability and imaging vessel wall inflammation in accordance with the present invention will help rapidly identify patients at high risk for acute coronary syndromes and stroke. In aortic aneurysm, imaging vessel wall inflammation will help identify patients who are at risk for aneurysm rupture or dissection. By binding and measuring integrins, especially including activated integrin pursuant to the present methods, inflammation can be measured and disease states can be assessed with a high degree of accuracy previously unavailable in the art.

Timely assessment and treatment of vascular disorders can prove critical to patient stabilization, recovery and survival, and the real time provision of *in vivo* vascular data to healthcare professionals through use of the invention facilitates the selection of treatment modalities that are most appropriate for the precise disease state condition presented.

These and other aspects of the invention are described further in the Detailed Description of the Invention.

Brief Description of the Figures

Figure 1. Flow cytometric assessment of $\alpha_v\beta_3$ expression and activation in monocytes and macrophages. a) Representative histograms of $\alpha_v\beta_3$ (top row) and RGD (bottom row) immunostaining of monocytes and monocyte-derived macrophages. b) Representative contour plots demonstrating co-staining of monocytes with anti- $\alpha_v\beta_3$ antibody and RGD peptide. ab: antibody, ctrl: control, RGD: fluorescent homologue of NC100691.

Figure 2. MicroSPECT/CT imaging of $\alpha_v\beta_3$ activation in vascular inflammation. a) Examples of contrast-enhanced CT and NC100692 microSPECT-CT fused images of an $apoE^{-/-}$ mouse 4 weeks after surgery to induce left common carotid artery vascular inflammation. Arrows point to common carotid arteries. R: right, L: left, T: transverse, C: coronal, S: sagittal, cpv: counts per voxel. b) MicroSPECT-derived quantification of NC100692 uptake in remodeling left and sham-operated right common carotid artery at 2 (n=9) and 4 (n=8) weeks after surgery. *: $p<0.001$.

Figure 3. NC100692 uptake specificity in vascular inflammation. MicroSPECT derived quantification of NC100692 signal in remodeling carotid artery in animals without (n=9) or with (n=3) injection with 50-fold excess unlabeled precursor prior to tracer administration. *: $p=0.004$, cpv: counts per voxel.

Figure 4. Inflammation-induced vascular remodeling in carotid arteries. a) examples of hematoxylin and eosin staining of $CaCl_2$-exposed left (L) and NaCl-exposed right (R) carotid arteries at 4 weeks after surgery demonstrating considerable remodeling of the left carotid artery. Scale bar: 100μm, b) Morphometric analysis of total vessel area of common carotid arteries at 4 weeks after surgery, n=8, *: $p<0.0001$.

Figure 5. Representative examples of macrophage (F 4/80) and α_v immunostaining (in red) of control right and remodeling left carotid arteries at 4 weeks after surgery. Nuclei are stained with DAPI in blue and elastic membrane autofluorescence is seen in green. L: lumen, Scale bar: 20 μm.

Figure 6. Gene expression in carotid arteries at 4 weeks after surgery. a) GAPDH-normalized smooth muscle α-actin, CD31, CD68, and EMR-1 mRNA expression in

control right and remodeling left carotid arteries detected by real time RT-PCR. n=8, *:p<0.05, **:p.0.01. b) GAPDH-normalized integrin mRNA expression in control right and remodeling left carotid arteries detected by real time RT-PCR demonstrating no significant difference. n=8.

Figure 7. Vascular inflammation and integrin $\alpha_v\beta_3$ tracer uptake in carotid arteries. There is a significant correlation between CD68 expression and NC100692 uptake in the same animal. Pearson's r = 0.67, p = 0.02.

Supplemental Figure 1. Flow cytometric assessment of $\alpha_v\beta_3$ activation in endothelial cells. RGD: fluorescent homologue of NC100691.

Supplemental Figure 2. Representative examples of CD31 (EC) and smooth muscle α-actin immunostaining (in red) of control right and remodeling left carotid arteries at 4 weeks after surgery. Nuclei are stained with DAPI in blue and elastic membrane autofluorescence is seen in green. L: lumen. Scale bar: 20 μm.

Detailed Description of the Invention

It is noted that, as used in this specification and the appended claims, the singular forms "a," "an," and "the," include plural referents unless expressly and unequivocally limited to one referent. Thus, for example, reference to "a compound" includes two or more different compounds. As used herein, the term "include" and its grammatical variants are intended to be non-limiting, such that recitation of items in a list is not to the exclusion of other like items that can be substituted or other items that can be added to the listed items.

The term "assessing" is used to describe a method of diagnosis or alternatively, a method of imaging useful in diagnosis.

The term "vascular remodeling" refers to a persistent change in the structure or composition of blood vessels. This term is used to describe the changes in size, shape, composition and function of arteries which occurs as a consequence of cardiovascular disease, often atherosclerosis and/or high blood pressure. The vascular (arterial) wall is an active, integrated organ composed of endothelial, smooth-muscle, and fibroblast cells

coupled to each other in a complex set of interactions. The vasculature is capable of sensing changes within its milieu, integrating these signals by intercellular communication, and changing itself through the local production of mediators that influence structure as well as function. Vascular remodeling is an active process of structural alteration that involves changes in at least four cellular processes – including cell growth, cell death, cell migration, and production or degradation of extracellular matrix.

An important concept for vascular remodeling, is Glagov's phenomenon, the observation that arteries remodel to maintain constant flow despite increases in atherosclerotic lesion mass. Although this phenomenon was originally described only for the case of arterial remodeling in response to growth of atherosclerotic plaques, experimental and clinical observations indicate that blood flow properties influence remodeling after angioplasty, hypertension, and flow diversion as well as atherosclerotic plaque progression.

Remodeling of large and small arteries often occurs as a response to blood flow, which is influenced by atheroslerosis, angioplasty, hypertension and flow diversion. In hypertension, changes in small artery structure are basically of 2 kinds: (1) inward or outward remodeling, in which outer and lumen diameters are decreased, media/lumen ratio are decreased or increased, and cross-sectional area of the media is unaltered; and (2) hypertrophic remodeling, in which the media thickens to encroach on the lumen, resulting in increased media cross-sectional area and media/lumen ratio. Cell growth, apoptosis, inflammation, and fibrosis contribute to vascular remodeling in hypertension. Apoptosis has been reported in hypertension to be both increased and decreased in different tissues, including blood vessels. Inflammation, which may be low grade, probably plays an important role in triggering fibrosis in cardiovascular disease and hypertension. Vascular fibrosis entails accumulation of collagen, fibronectin, and other extracellular matrix components in the vessel wall and is an important aspect of extracellular matrix remodeling in hypertension. Associated with this, there may be increases in cell-matrix attachment sites and changes in their topographical localization that may modulate arterial structure. Imbalance in matrix metalloproteinase/tissue inhibitors of metalloproteinases may contribute to alteration in collagen turnover and extracellular matrix remodeling. Chronic vasoconstriction may lead to embedding of the contracted vessel structure in a remodeled extracellular matrix, contributing to the inward remodeling of the blood vessel as smooth muscle cells are rearranged around a smaller lumen. Alternatively, there may be outward

remodeling. The resulting remodeling of small arteries may initially be adaptive, but eventually it becomes maladaptive and compromises organ function, contributing to cardiovascular complications of hypertension and other cardiovascular disease states.

In the present invention, assessment (including diagnosis, evaluation of, prognosis and progression) of vascular remodeling is performed using standard methods where data obtained from a patient is compared to a control (as otherwise defined herein) which provides a standard upon which a comparison between the patient data and one or more control(s) may be made (typically by an attending physician or other medical professional) in order to determine whether or not the patient likely exhibits or will likely exhibit vascular remodeling. The data can provide an assessment of the extent of vascular remodeling, a prognosis for future remodeling and if present, the extent of cardiovascular disease and/or the likelihood of future cardiovascular disease. This is determined by a comparison between the data obtained from the patient or subject and a control value which is established from one or more healthy patients and/or one or more patients (or groups of patients) in which vascular remodeling and/or cardiovascular disease is present. A determination in a patient of the presence or absence of vascular remodeling and/or the likelihood of future vascular remodeling and/or the presence or absence of cardiovascular disease is made based upon the comparison between the data obtained from the patient and the control value(s). Appropriate therapy will follow based upon the assessment made.

Because arterial remodeling is a dynamic phenomenon that takes place in aneurysm, transplant vasculopathy (chronic graft rejection) and alongside atherosclerotic plaque development, with early, softer plaques causing positive remodeling and older, harder plaques associated with negative remodeling, it is a particularly useful analytical tool for assessing cardiovascular disease. Thus, assessing vascular remodeling is a particularly useful tool for assessing coronary and aortic pathophysiology consistent with cardiovascular disease.

"Integrins" are a superfamily of cell adhesion receptors, which exist as heterodimeric transmembrane glycoproteins. They are part of a large family of cell adhesion receptors which are involved in cell-extracellular matrix and cell-cell interactions. Integrins play critical roles in cell adhesion to the extracellular matrix (ECM) which, in turn, mediates cell survival, proliferation and migration through intracellular signaling. The receptors consist of two subunits that are non-covalently bound. Those subunits are called alpha and beta. The

alpha subunits all have some homology to each other, as do the beta subunits. The receptors always contain one alpha chain and one beta chain and are thus called heterodimeric. Both of the subunits contribute to the binding of ligand. Eighteen alpha subunits and eight beta subunits have been identified, which heterodimerize to form at least twenty-four distinct integrin receptors.

Among the variety of alpha chain subunits is a protein chain referred to as alpha V (α_v). The ITAGV gene encodes integrin α_v. The I-domain containing integrin α_v undergoes post-translational cleavage to yield disulfide-linked heavy and light chains, that combine with multiple integrin β chains to form different integrins. Alternative splicing of the gene yields seven different transcripts; a, b, c, e, f, h, j, which together encode six different protein isoforms of α_v. Among the known associating β chains (β chains 1, 3, 5, 6, and 8 (ITG β_1, ITG β_3, ITG β_5, ITG β_6, and ITG β_8), each can interact with extracellular matrix ligands. The $\alpha_v\beta_3$ integrin, perhaps the most studied of these, is referred to as the vitronectin receptor (VNR). In addition to providing for cell attachment to other cells or to extracellular proteins such as vitronectin ($\alpha_v\beta_3$) and fibronectin ($\alpha_v\beta_6$), the integrins are capable of intracellular signaling which provides clues for cell migration and secretion of or elaboration of other proteins involved in cell motility and invasion and angiogenesis. The α_v integrin subfamily of integrins recognize the ligand motif arg-gly-asp (RGD) present in fibronectin, vitronectin, VonWillebrand factor, fibrinogen and other proteins.

Those of ordinary skill in the art are able to make a wide variety of ligands (e.g. peptide mimetics and antibodies) having a binding affinity for αvβ3 integrin without undue experimentation, and the ligands described herein are purely illustrative and in no way limiting. As explained above, and as elaborated on in the following excerpts from Chen, Integrin Targeted Delivery of Chemotherapeutics, Theranostics. 2011; 1: 189–200 (Chen), "the arginine-glycine-aspartic acid (RGD) cell adhesion sequence was discovered in fibronectin. Proteins that contain the RGD attachment site, together with the integrins that serve as receptors for them, constitute a major recognition system for cell adhesion. The RGD sequence is the cell attachment site of a number of adhesive ECM, blood, and cell surface proteins. It has been found that nearly half of the over 20 known integrins, including all five αv integrins, two β1 integrins (α5, α8) and αIIbβ3 integrin, recognize this sequence in their adhesion protein ligands. The integrin αvβ3, consists of a 125-kDa αv subunit and a 105-kDa β3 subunit, and binds a wide range of ECM proteins with RGD-containing components of the

interstitial matrix such as vitronectin, fibronectin and thrombospondin. RGD binds at an interface between the α and β subunits, the R residue fitting into a cleft in a β-propeller module in the subunit, and the D coordinating a cation bound in a von Willebrand factor A - domain in the β subunit."

As explained further by Chen, RGD-peptides can be served as vectors for integrin αvβ3 targeted delivery of chemotherapeutics. Cyclic peptides c(RGDfK) and c(RGDyK) are the ones mostly used for the delivery of therapeutic agents. The amino group of the lysine residue on these peptides is an ideal site for further chemical conjugation reactions. Multivalent c(RGDfK) or c(RGDyK) peptide can be used to achieve higher binding affinity.

Consequently, a wide variety of detectable ligands having a binding affinity for $\alpha_v\beta_3$ integrin may be used in the methods of the invention, including but not limited to labeled NC100692, or alternatively, detectable versions of the antibodies disclosed in United States Patent No. 6,171,588, Vitaxin (humanized antibody composed of human IgG-1, kappa, and the complement domain regions of the murine antibody LM 609), Vitaxin-2–conjugated, gadolinium-encapsulated nanoparticles and other detectable monoclonal $\alpha_v\beta_3$ integrin antibodies, detectable versions of the small molecule $\alpha_v\beta_3$ integrins disclosed in or incorporated by reference in United States Patent No. 7,566,442, and detectable naturally occurring or synthetic peptides and small-molecule peptidomimetics (often preferred) including but not limited to ^{111}In-MSAP-RGD, (^{18})F-galacto-RGD, ((^{18})F-RGD, (^{18})F-AlF-NOTA-PRGD2, [(99m)Tc]HYNIC-RGD [6-hydrazinonicotinic acid conjugated to cyclo(Arg-Gly-Asp-D-Phe-Lys), (^{99m})Tc-RAFT-RAD, (^{64})Cu-RGD, (^{18})F-galacto-RGD, (^{99m})Tc-RAFT-RAD, ^{18}F-FBEM. [^{18}F]fluciclatide, ^{111}In-labeled 1,4,7,10-tetraazacyclododecane-1,4,7,10-tetracetic acid (DOTA)-Glu{PEG4-Glu[cyclo(Lys(Gly-Gly-Gly)-Arg-Gly-Asp-d-Phe)]-cyclo(Lys(Gly-Gly-Gly)-Arg-Gly-Asp-d-Phe)}-{PEG4-Glu[cyclo(Lys(Gly-Gly-Gly)-Arg-Gly-Asp-d-Phe)]-cyclo(Lys(Gly-Gly-Gly)-Arg-Gly-Asp-d-Phe)}, abbreviated as ^{111}In(DOTA-2P4G-RGD4) or ^{111}In-DOTA-E{PEG4-E[Gly3-c(RGDfK)]2}2; RGD multimers such as those disclosed or referenced in Shan, Molecular Imaging and Contrast Agent Database (MICAD) [Internet]. Bethesda (MD): National Center for Biotechnology Information (US); 2004-2011.2012 Feb 23; RGD4C/Cy5.5-ferritin ^{64}Cu-loaded nanocages (RGD4C/Cy5.5-Fn-^{64}Cu nanocages); nanoshell (NS)-RGDfK, cyclic peptide LXW7, and 3-substituted tetrahydro-[1,8]naphthyridine–containing αvβ3 antagonists and other detectable ligands specific for $\alpha_v\beta_3$ integrin as disclosed or referenced in Shan,

Molecular Imaging and Contrast Agent Database (MICAD) [Internet]. Bethesda (MD): National Center for Biotechnology Information (US); 2004-2010. (2010 Jan 06). The use of labeled NC100692 and related labeled RGD peptides which can bind selectively to activated integrin is preferred.

"Activated integrin" is a term used to describe an integrin in a high affinity state (exhibiting a conformational change consistent with its activated state) that can be distinguished by virtue of its modified conformation (relative to an inactive integrin) and can be monitored in vascular tissue to provide insight into inflammatory processes associated with numerous vascular disease states as otherwise described herein, especially including atherosclerosis and aortic aneurysm, vasculitis and transplant vasculopathy (chronic allograft rejection). While not being limited by way of theory, it is believed that activated integrin binds to vascular tissue pursuant to an upregulated inflammatory process as disease states progress, thus providing a target for binding and insight into the inflammatory process and consequently the disease states in vascular tissue.

"Image" or "imaging" broadly refers to both viewable images and data representing a viewable image. Preferred embodiments generate, or are configured to generate, at least one viewable image. Useful imaging systems include but are not limited to Positron Emission Tomography (PET), a Single Photon Emission Computed Tomography (SPECT), Computed Tomography (CT), ultrasonography, Magnetic Resonance Imaging (MRI) or any other system capable or generating tomographic or planar images.

The PET imaging technique was developed in the 1970's primarily for brain imaging research. In 1998, the Centers for Medicare and Medicaid Services approved ^{18}F-FDG PET for use in specific clinical applications, such as primary pulmonary tumor staging. The use and availability of ^{18}F-FDG PET has grown with its utility in oncology imaging. In 2004, the Centers for Medicare and Medicaid Services approved ^{18}F-FDG PET imaging for the evaluation of both FTD and AD.

The most common radiotracer in clinical PET imaging is ^{18}F-FDG. ^{18}F-FDG crosses the blood-brain barrier through a glucose transporter and is transported into the cells by another glucose transport protein, glucose transporter 1. Inside the cell, ^{18}F-FDG and glucose

are substrates for hexokinase, undergoing phosphorylation. Unlike glucose, ^{18}F-FDG cannot continue down the glucose pathway and is subsequently "trapped" within the cell.

"Near-infrared (NIR) fluorescence detection" is well-known to those of ordinary skill in the art. As explained in Rao, *et al.*, Fluorescence imaging in vivo: recent advances" *Current Opinions Biotechnol.*, 2007 Feb;18(1):17-25, *"in vivo* fluorescence imaging uses a sensitive camera to detect fluorescence emission from fluorophores in whole-body living small animals. To overcome the photon attenuation in living tissue, fluorophores with long emission at the near-infrared (NIR) region are generally preferred, including widely used small indocarbocyanine dyes." The technique of NIR is adaptable to human patients through invasive intravascular detection.

As used herein, "antibody" includes, but is not limited to, monoclonal antibodies. The following disclosure from U.S. Patent Application Document No. 20100284921, the entire contents of which are hereby incorporated by reference, exemplifies techniques that are useful in making antibodies employed in formulations of the instant invention.

As described in U.S. Patent Application Document No. 20100284921, "antibodies...may be polyclonal or monoclonal. Monoclonal antibodies are preferred. The antibody is preferably a chimeric antibody. For human use, the antibody is preferably a humanized chimeric antibody.

An anti-target-structure antibody ... may be monovalent, divalent or polyvalent in order to achieve target structure binding. Monovalent immunoglobulins are dimers (HL) formed of a hybrid heavy chain associated through disulfide bridges with a hybrid light chain. Divalent immunoglobulins are tetramers (H2L2) formed of two dimers associated through at least one disulfide bridge.

The invention also includes [use of] functional equivalents of the antibodies described herein. Functional equivalents have binding characteristics comparable to those of the antibodies, and include, for example, hybridized and single chain antibodies, as well as fragments thereof. Methods of producing such functional equivalents are disclosed in PCT Application Nos. WO 1993/21319 and WO 1989/09622. Functional equivalents include polypeptides with amino acid sequences substantially the same as the amino acid sequence of

the variable or hypervariable regions of the antibodies raised against target $\alpha_v\beta_3$ integrin according to the practice of the present invention.

Functional equivalents of the anti-target-structure antibodies further include fragments of antibodies that have the same, or substantially the same, binding characteristics to those of the whole antibody. Such fragments may contain one or both Fab fragments or the $F(ab')_2$ fragment. Preferably the antibody fragments contain all six complement determining regions of the whole antibody, although fragments containing fewer than all of such regions, such as three, four or five complement determining regions, are also functional. The functional equivalents are members of the IgG immunoglobulin class and subclasses thereof, but may be or may combine any one of the following immunoglobulin classes: IgM, IgA, IgD, or IgE, and subclasses thereof. Heavy chains of various subclasses, such as the IgG subclasses, are responsible for different effector functions and thus, by choosing the desired heavy chain constant region, hybrid antibodies with desired effector function are produced. Preferred constant regions are gamma 1 (IgG1), gamma 2 (IgG2 and IgG), gamma 3 (IgG3) and gamma 4 (IgG4). The light chain constant region can be of the kappa or lambda type.

The monoclonal antibodies may be advantageously cleaved by proteolytic enzymes to generate fragments retaining the target structure binding site. For example, proteolytic treatment of IgG antibodies with papain at neutral pH generates two identical so-called "Fab" fragments, each containing one intact light chain disulfide-bonded to a fragment of the heavy chain (Fc). Each Fab fragment contains one antigen-combining site. The remaining portion of the IgG molecule is a dimer known as "Fc". Similarly, pepsin cleavage at pH 4 results in the so-called F(ab')2 fragment.

Single chain antibodies or Fv fragments are polypeptides that consist of the variable region of the heavy chain of the antibody linked to the variable region of the light chain, with or without an interconnecting linker. Thus, the Fv comprises an antibody combining site.

Hybrid antibodies may be employed. Hybrid antibodies have constant regions derived substantially or exclusively from human antibody constant regions and variable regions derived substantially or exclusively from the sequence of the variable region of a monoclonal antibody from each stable hybridoma.

Methods for preparation of fragments of antibodies (e.g. for preparing an antibody or an antigen binding fragment thereof having specific binding affinity for a target antigen are either described in the experiments herein or are otherwise known to those skilled in the art. See, Goding, "Monoclonal Antibodies Principles and Practice", Academic Press (1983), p. 119-123. Fragments of the monoclonal antibodies containing the antigen binding site, such as Fab and F(ab')2 fragments, may be preferred in therapeutic applications, owing to their reduced immunogenicity. Such fragments are less immunogenic than the intact antibody, which contains the immunogenic Fc portion. Hence, as used herein, the term "antibody" includes intact antibody molecules and fragments thereof that retain antigen binding ability.

When the antibody used in the practice of the invention is a polyclonal antibody (IgG), the antibody is generated by inoculating a suitable animal with a target structure or a fragment thereof. Antibodies produced in the inoculated animal that specifically bind the target structure are then isolated from fluid obtained from the animal. Anti-target-structure antibodies may be generated in this manner in several non-human mammals such as, but not limited to, goat, sheep, horse, rabbit, and donkey. Methods for generating polyclonal antibodies are well known in the art and are described, for example in Harlow et al. (In: Antibodies, A Laboratory Manual, 1988, Cold Spring Harbor, N.Y.).

When the antibody used in the methods used in the practice of the invention is a monoclonal antibody, the antibody is generated using any well known monoclonal antibody preparation procedures such as those described, for example, in Harlow et al. (supra) and in Tuszynski et al. (Blood 1988, 72:109-115). Generally, monoclonal antibodies directed against a desired antigen are generated from mice immunized with the antigen using standard procedures as referenced herein. Monoclonal antibodies directed against full length or fragments of target structure may be prepared using the techniques described in Harlow et al. (supra).

The effects of sensitization in the therapeutic or diagnostic use of animal-origin monoclonal antibodies in the treatment or diagnosis of human disease may be diminished by employing a hybrid molecule generated from the same Fab fragment, but a different Fc fragment, than contained in monoclonal antibodies previously administered to the same subject. It is contemplated that such hybrid molecules formed from the anti-target-structure monoclonal antibodies may be used in the present invention. The effects of sensitization are

further diminished by preparing animal/human chimeric antibodies, e.g., mouse/human chimeric antibodies, or humanized (i.e. CDR-grafted) antibodies. Such monoclonal antibodies comprise a variable region, i.e., antigen binding region, and a constant region derived from different species. By 'chimeric' antibody is meant an antibody that comprises elements partly derived from one species and partly derived form at least one other species, e.g., a mouse/human chimeric antibody.

Chimeric animal-human monoclonal antibodies may be prepared by conventional recombinant DNA and gene transfection techniques well known in the art. The variable region genes of a mouse antibody-producing myeloma cell line of known antigen-binding specificity are joined with human immunoglobulin constant region genes. When such gene constructs are transfected into mouse myeloma cells, the antibodies produced are largely human but contain antigen-binding specificities generated in mice. As demonstrated by Morrison et al., 1984, Proc. Natl. Acad. Sci. USA 81:6851-6855, both chimeric heavy chain V region exon (VH)-human heavy chain C region genes and chimeric mouse light chain V region exon (VK)-human K light chain gene constructs may be expressed when transfected into mouse myeloma cell lines. When both chimeric heavy and light chain genes are transfected into the same myeloma cell, an intact H2L2 chimeric antibody is produced. The methodology for producing such chimeric antibodies by combining genomic clones of V and C region genes is described in the above-mentioned paper of Morrison et al., and by Boulianne et al. (Nature 1984, 312:642-646). Also see Tan et al. (J. Immunol. 1985, 135:3564-3567) for a description of high level expression from a human heavy chain promotor of a human-mouse chimeric K chain after transfection of mouse myeloma cells. As an alternative to combining genomic DNA, cDNA clones of the relevant V and C regions may be combined for production of chimeric antibodies, as described by Whitte et al. (Protein Eng. 1987, 1:499-505) and Liu et al. (Proc. Natl. Acad. Sci. USA 1987, 84:3439-3443). For examples of the preparation of chimeric antibodies, see the following U.S. Pat. Nos 5,292,867; 5,091,313; 5,204,244; 5,202,238; and 5,169,939. The entire disclosures of these patents, and the publications mentioned in the preceding paragraph, are incorporated herein by reference. Any of these recombinant techniques are available for production of rodent/human chimeric monoclonal antibodies against target structures.

To further reduce the immunogenicity of murine antibodies, "humanized" antibodies have been constructed in which only the minimum necessary parts of the mouse antibody, the

complementarity-determining regions (CDRs), are combined with human V region frameworks and human C regions (Jones et al., 1986, Nature 321:522-525; Verhoeyen et al., 1988, Science 239:1534-1536; Hale et al., 1988, Lancet 2:1394-1399; Queen et al., 1989, Proc. Natl. Acad. Sci. USA 86:10029-10033). The entire disclosures of the aforementioned papers are incorporated herein by reference. This technique results in the reduction of the xenogeneic elements in the humanized antibody to a minimum. Rodent antigen binding sites are built directly into human antibodies by transplanting only the antigen binding site, rather than the entire variable domain, from a rodent antibody. This technique is available for production of chimeric rodent/human anti-target structure antibodies of reduced human immunogenicity."

Further, standard techniques for growing cells, separating cells, and where relevant, cloning, DNA isolation, amplification and purification, for enzymatic reactions involving DNA ligase, DNA polymerase, restriction endonucleases and the like, and various separation techniques are those known and commonly employed by those skilled in the art. A number of standard techniques are described in Sambrook *et al.*, 1989 Molecular Cloning, Second Edition, Cold Spring Harbor Laboratory, Plainview, New York; Maniatis *et al.*, 1982 Molecular Cloning, Cold Spring Harbor Laboratory, Plainview, New York; Wu (Ed.) 1993 Meth. Enzymol. 218, Part I; Wu (Ed.) 1979 Meth. Enzymol. 68; Wu et al., (Eds.) 1983 Meth. Enzymol. 100 and 101; Grossman and Moldave (Eds.) 1980 Meth. Enzymol. 65; Miller (ed.) 1972 Experiments in Molecular Genetics, Cold Spring Harbor Laboratory, Cold Spring Harbor, New York; Old and Primrose, 1981 Principles of Gene Manipulation, University of California Press, Berkeley; Schleif and Wensink, 1982 Practical Methods in Molecular Biology; Glover (Ed.) 1985 DNA Cloning Vol. I and II, IRL Press, Oxford, UK; Hames and Higgins (Eds.) 1985 Nucleic Acid Hybridization, IRL Press, Oxford, UK; and Setlow and Hollaender 1979 Genetic Engineering: Principles and Methods, Vols. 1-4, Plenum Press, New York. Abbreviations and nomenclature, where employed, are deemed standard in the field and commonly used in professional journals such as those cited herein.

In certain embodiments, a "detectable ligand having a binding affinity for $\alpha_v\beta_3$ integrin" is comprised of an $\alpha_v\beta_3$ integrin antibody derivatized with or linked to a detectable moiety selected from the group consisting of:

(a) a fluorescent label or fluorescer including but not limited to fluorescein and its derivatives, fluorochrome, GFP (Green Fluorescent Protein), dansyl, umbelliferone, phycoerythrin, phycocyanin, allophycocyanin, o-phthaldehyde, fluorescamine; a fluorophore lanthanide cryptates, a chelate, a chemoluminescent label, the chemiluminescers isoluminol and luminol and a dioxetane;

(b) the bio-luminescent labels including but not limited to luciferase and luciferin;

(c) a sensitizer, e.g. any moiety which, when stimulated by excitation with radiation of one or more wavelengths or other chemical or physical stimulus (e.g., electron transfer, electrolysis, electroluminescence or energy transfer), will achieve an excited state which upon interaction with molecular oxygen will produce singlet molecular oxygen, or upon interaction with a leucodye will assume a reduced form which can then be returned to its original unexcited state by interaction with molecular oxygen resulting in the production of hydrogen peroxide (Y and Gd-containing sensitizers are preferred);

(d) a coenzyme or enzyme substrates including but not limited to alkaline phosphatase, glucose-6-phosphate dehydrogenase (G6PDH), alpha-D-galactosidase, glucose oxydase, glucose amylase, carbonic anhydrase, acetylcholinesterase, lysozyme, malate dehydrogenase, lysozyme, peroxidase, and horseradish peroxidase;

(e) a radiolabel may include but is not limited to ^{18}fluorine, ^{64}copper, ^{65}copper, ^{11}carbon, ^{14}carbon, ^{67}gallium, ^{68}gallium, ^{77}bromine, ^{80m}bromine, ^{95}ruthenium, ^{97}ruthenium, ^{103}ruthenium, ^{105}ruthenium, ^{99m}technetium, ^{107}mercury, ^{203}mercury, ^{123}iodine, ^{124}iodine, ^{125}iodine, ^{126}iodine, ^{131}iodine, ^{133}iodine, ^{111}Indium, ^{113}mindium, ^{99m}rhenium, ^{105}rhenium, ^{101}rhenium, ^{186}rhenium, ^{188}rhenium, ^{121}mtellurium, ^{99}technetium, ^{122m}tellurium, ^{125m}tellurium, ^{165}thulium, ^{167}thulium, ^{168}thulium, ^{90}yttrium, and nitride or oxide forms derived thereof. Preferably, ^{18}fluorine, ^{64}copper, ^{65}copper, ^{11}carbon, ^{67}gallium, ^{68}gallium, ^{77}bromine, ^{80m}bromine, ^{123}iodine, ^{124}iodine, ^{125}iodine, ^{126}iodine, ^{133}iodine, ^{111}Indium, and nitride or oxide forms derived thereof are used;

(f) a radiolabel selected from the group consisting of the alpha emitters ^{213}bismuth, ^{213}lead and ^{225}actinium;

(g) labelled avidin or streptavidin;

(h) a latex or carbon particle (e.g. colored latex particles, platinized carbon particles, nanparticle versions thereof, etc.); and

(i) biotin, digoxygenin or 5-bromodeoxyuridine.

An $\alpha_v\beta_3$ integrin antibody, peptide, or peptide mimetic can be derivatized with or linked to a detectable moiety in a wide variety of ways. For example, the $\alpha_v\beta_3$ integrin antibody, peptide, or peptide mimetic is linked to the detectable moiety by a linker including but not limited to diethylenetriamine pentaacetate (DTPA)-isothiocyanate, succinimidyl 6-hydrazinium nicotinate hydrochloride (SHNH), and hexamethylpropylene amine oxime (HMPAO). Also, the $\alpha_v\beta_3$ integrin antibody can be derivatized at a cysteine residue with a radiolabel detectable moiety. A chelator can be used to mediate binding of the $\alpha_v\beta_3$ integrin antibody to the radiolabel detectable moiety. All of these techniques are purely illustrative, and those of ordinary skill in the art will appreciate that a wide range of alternative approaches are available to derivatize with or link a detectable moiety to a $\alpha_v\beta_3$ integrin antibody.

In certain embodiments, an increase of about 100%, 95%, 90%, 85%, 80%, 75%, 70%, 65%, 60%, 55%, 50%, 45%, 40%, 35%, 30%, 25%, 20%, 15%, 10%, 9%, 8%, 7%, 6%, 5%, 4%, 3%, 2% or 1% in the subject's vascular uptake of the labeled ligand when compared to the standard or control sample indicates that the subject suffers from, or is risk of developing, a vascular disease.

In certain embodiments, a decrease of about 100%, 95%, 90%, 85%, 80%, 75%, 70%, 65%, 60%, 55%, 50%, 45%, 40%, 35%, 30%, 25%, 20%, 15%, 10%, 9%, 8%, 7%, 6%, 5%, 4%, 3%, 2% or 1% in the vascular uptake of the labeled ligand in a subject being treated for a vascular disease when compared to the standard or control sample indicates treatment efficacy.

Measuring vascular inflammation and integrin $\alpha_v\beta_3$ tracer uptake in, for example, carotid arteries in accordance with the invention can be accomplished in any number of ways. In an illustrative example which includes both preclinical and clinical imaging aspects, $\alpha_v\beta_3$ integrin antibody, peptide, or peptide mimetic is administered a mouse with carotid artery

aneurysm and the mouse is imaged after 2 hours using a high-resolution imaging system (X-SPECT, Gamma Medica-Ideas, Northridge, CA) with 1-mm medium-energy collimators. Three point sources of known activities (37 to 185 kBq) are placed in the field of view but outside the body to quantify uptake and to verify the accuracy of image fusion. The following acquisition parameters are used for microSPECT imaging: 360 degree, 128 projections, 30 seconds/projection (~80 minute image acquisition), with 174 and 242 keV photopeaks ±10% window (for ^{111}In). After completion of microSPECT imaging, the patient is injected with a continuous infusion of iodinated CT contrast (iohexol 100 μL/min) over 2 minutes, and CT imaging is performed (energy 75 kVp/280 μA, matrix 512×512) to identify anatomic structure. The imaging protocol lasts ~1.5 hour, after which time (3.5 hours after tracer administration) different tissues are optionally harvested for autoradiography or gamma-well counting. Imaging with RP805 (^{99}Tc-labeledcan also be used. Fenestra (200μl, ART Advanced Research Technologies, Montreal, QC, Canada) can be used as a CT contract agent. The imaging protocol is similar to RP782 with the exception of the low-energy pinhole collimators and 140 Kev photopeak ±10% window is for ^{99m}Tc imaging. For quantitative analysis of tracer uptake, cylindrical regions of interest (ROIs) are drawn at the level of carotid artery bifurcation (2×2×2 mm). A ROI immediately posterior to both carotids is used to calculate the background activity. Data is expressed as background-corrected cpv/MBq injected.

In an illustrative example of vascular wall remodeling that may be detected or further predicted using the methods of the invention, an arterial aneurysm can lead to progressive expansion of the artery over a period of several weeks. Demonstrated straightening of elastic laminae and areas of discontinuity can progress to almost complete dissolution of membranes after several weeks. The cross-sectional area of left carotid arteries is significantly higher than control right carotid arteries (e.g. 0.26±0.05 mm^2 versus 0.10±0.01 mm^2, or e.g. 0.30±0.03 mm^2 versus 0.09±0.01 mm^2, or e.g. 0.55±0.11 mm^2 versus 0.12±0.01 mm^2.

Similar illustrative protocols and related values are present in Example 1 hereinafter. As shown in Example 1 hereinafter, macrophage content of a vessel wall can also quantified by real time RT-PCR and will likely show significantly higher levels of GAPDH-normalized CD68 and EMRI mRNA expression in injured, as compared to control arteries.

In certain non-limiting embodiments, an increase in a subject's vascular uptake of a labeled ligand when compared to the standard or control sample, or a change in vascular remodeling when compared to a control, can reflect an increase or a decrease in a subject or test sample of the level of vascular uptake of a labeled ligand or vascular remodeling as compared to a comparable level of measured vascular uptake of a labeled ligand or vascular remodeling in a control subject or sample can be an increase or decrease in the magnitude of approximately ± 5,000-10,000%, or approximately ± 2,500-5,000%, or approximately ± 1,000-2,500%, or approximately ± 500-1,000%, or approximately ± 250-500%, or approximately ± 100-250%, or approximately ± 50-100%, or approximately ± 25-50%, or approximately ± 10-25%, or approximately ± 10-20%, or approximately ± 10-15%, or approximately ± 5-10%, or approximately ± 1-5%, or approximately ± 0.5-1%, or approximately ± 0.1-0.5%, or approximately ± 0.01-0.1%, or approximately ± 0.001-0.01%, or approximately ± 0.0001-0.001%.

The values obtained from controls are reference values representing a known health status and the values obtained from test samples or subjects are reference values representing a known disease status or a state of vascular remodeling. The term "control", as used herein, can mean a sample of preferably the same source (e.g. blood vessels, blood, serum, tissue etc.) which is obtained from at least one healthy subject to be compared to the sample to be analyzed. In order to receive comparable results the control as well as the sample should be obtained, handled and treated in the same way. In certain examples, the number of healthy individuals used to obtain a control value may be at least one, preferably at least two, more preferably at least five, most preferably at least ten, in particular at least twenty. However, the values may also be obtained from at least one hundred, one thousand or ten thousand individuals. Any one or more of the disease states or conditions which are identified herein may have a specific control which may be used for purposes of assessing cardiovascular disease or therapeutic intervention or alternatively, vascular remodeling, etc. by the present method.

In the case of vascular remodeling, numerous publications have documented patient characteristics and clinical conditions associated with a particular type of remodeling, thus providing a basis for establishing controls useful in assessing vascular remoding in a patient. . See, for example, Weissman, et al.,. *Am J Cardiol.* 1999;84:37–40; Schoenhagen, et al. *Circulation.* 2000;101:598–603; Varnava, *Circulation.* 2002;105:939–943 and Davies, et al.,

Heart. 2000;84:461–462. Remodeling has even been reported in arterialized saphenous vein grafts, See, Mendelsohn, et al., *Am J Cardiol.* 1995;76:1066–1069.

In the steps of comparing measurements of a subject's vascular uptake of a detectable ligand to a first standard or control, and optionally comparing vascular wall remodeling to a second standard or control, the first and second standards and controls can be the same or different. For example, the first standard or control could be data reflective of an average rate at which vascular tissue samples obtained from a cross-section of healthy human volunteers uptake $\alpha_v\beta_3$ integrin antibody, and the second standard or control could be data reflective of an average arterial cross-section and macrophage content of arterial samples obtained from a cross-section of healthy human volunteers.

In certain embodiments, vascular tissue and/or cell samples are obtained from a subject undergoing diagnosis and/or treatment and these samples are analyzed for vascular disease-related morphological changes.

Exemplary high-throughput assay systems that can be used include, but are not limited to, an Applied Biosystems plate-reader system (using a plate with any number of wells, including, but not limited to, a 96-well plate, a-384 well plate, a 768-well plate, a 1,536-well plate, a 3,456-well plate, a 6,144-well plate, and a plate with 30,000 or more wells), the ABI 7900 Micro Fluidic Card system (using a card with any number of wells, including, but not limited to, a 384-well card), other microfluidic systems that exploit the use of TaqMan probes (including, but not limited to, systems described in WO 04083443 A1, and published U.S. Patent Application Nos. 2003-0138829 A1 and 2003-0008308 A1), other micro card systems (including, but not limited to, WO04067175 A1, and published U.S. Patent Application Nos. 2004-083443 A1, 2004-0110275 A1, and 2004-0121364 A1), the Invader® system (Third Wave Technologies), the OpenArray® system (Biotrove), systems including integrated fluidic circuits (Fluidigm), and other assay systems known in the art. In certain embodiments, multiple different labels are used in each multiplex amplification reaction in a high-throughput multiplex amplification assay system such that a large number of different target nucleic acid sequences can be analyzed on a single plate or card. In certain embodiments, a high-throughput multiplex amplification assay system is capable of analyzing most of the genes in a genome on a single plate or card. In certain embodiments, a high-throughput multiplex amplification assay system is capable of analyzing all genes in an

entire genome on a single plate or card. In certain embodiments, a high-throughput multiplex amplification assay system is capable of analyzing most of the nucleic acids in a transcriptome on a single plate or card. In certain embodiments, a high-throughput multiplex amplification assay system is capable of analyzing all of the nucleic acids in a transcriptome on a single plate or card.

The practice of the present invention may also employ conventional biology methods, software and systems. Computer software products of the invention typically include computer readable medium having computer-executable instructions for performing the logic steps of the method of the invention. Suitable computer readable medium include floppy disk, CD-ROM/DVD/DVD-ROM, hard-disk drive, flash memory, ROM/RAM, magnetic tapes and etc. The computer executable instructions may be written in a suitable computer language or combination of several languages. Basic computational biology methods are described in, for example Setubal and Meidanis et al., Introduction to Computational Biology Methods (PWS Publishing Company, Boston, 1997); Salzberg, Searles, Kasif, (Ed.), Computational Methods in Molecular Biology, (Elsevier, Amsterdam, 1998); Rashidi and Buehler, Bioinformatics Basics: Application in Biological Science and Medicine (CRC Press, London, 2000) and Ouelette and Bzevanis Bioinformatics: A Practical Guide for Analysis of Gene and Proteins (Wiley & Sons, Inc., 2.sup.nd ed., 2001). See U.S. Pat. No. 6,420,108.

The present invention may also make use of various computer program products and software for a variety of purposes, such as ligand design, management of data, analysis, and instrument operation. See, U.S. Pat. Nos. 5,593,839, 5,795,716, 5,733,729, 5,974,164, 6,066,454, 6,090,555, 6,185,561, 6,188,783, 6,223,127, 6,229,911 and 6,308,170.

Additionally, the present invention relates to embodiments that include methods for providing information over networks such as the Internet. For example, the components of the system may be interconnected via any suitable means including over a network, e.g. integration of PET with the processor or computing device. The processor may take the form of a portable processing device that may be carried by an individual user e.g. lap top, and data can be transmitted to or received from any device, such as for example, server, laptop, desktop, PDA, cell phone capable of receiving data, BLACKBERRY®, and the like. In some embodiments of the invention, the system and the processor may be integrated into a single unit. In another example, a wireless device can be used to receive information and forward it

to another processor over a telecommunications network, for example, a text or multi-media message.

The functions of the processor need not be carried out on a single processing device. They may, instead be distributed among a plurality of processors, which may be interconnected over a network. Further, the information can be encoded using encryption methods, e.g. SSL, prior to transmitting over a network or remote user. The information required for decoding the captured encoded images taken from test objects may be stored in databases that are accessible to various users over the same or a different network.

In some embodiments, the data is saved to a data storage device and can be accessed through a web site. Authorized users can log onto the web site, upload scanned images, and immediately receive results on their browser. Results can also be stored in a database for future reviews.

In some embodiments, a web-based service may be implemented using standards for interface and data representation, such as SOAP and XML, to enable third parties to connect their information services and software to the data. This approach would enable seamless data request/response flow among diverse platforms and software applications.

The term "patient" or "subject" refers to an animal, such as a mammal, or a human, in need of vascular diagnosis to which methods according to the present invention are administered in order to diagnose and facilitate the treatment of a condition or disease state associated with a vascular or vascular inflammation-associated disorder.

A "vascular disorder" includes but is not limited to ischemic stroke, hemorrhagic stroke, transient ischemic attack (TIA), vascular inflammation due to atherosclerosis, thrombi or emboli resulting from atherosclerosis, arteritis, physical obstruction of arterial blood supply to the brain, lacunar stroke, hypoperfusion emboding diffuse injury caused by non-localized cerebral ischemia, myocardial infarction and arrhythmia, restenosis associated with percutaneous transluminal coronary angioplasty, peripheral vascular disease and cerebral vascular disease, venous occlusive disorders such as deep vein thrombosis, hypercoagulopathies and aneurysms.

Chronic progressive vascular disease (CPVD) is also a "vascular disorder" as defined herein and is a complication of several of the most common diseases afflicting the developed world, including diabetes mellitus, hypertension, the various hyperlipidemias, and the like. The present therapeutic modalities dealing with CPVD are aimed at the underlying causes. Unfortunately, for the most part there are no known cures, or their control is very difficult to accomplish in the general population. In addition, CPVD is often not only well-established, but also far-advanced, by the time that the underlying cause(s) come to medical attention. Thus, one is left with attempting to treat secondary complications, of which CPVD is the most serious because it leads to renal failure, strokes, heart disease and blindness.

Generally, CPVD is characterized by a change in vascular smooth muscle cells. One of the major changes is an increase in the amount and alteration of the types of connective tissue that they synthesize. This results in scarring and marked changes in function. In blood vessels, this leads to loss of elasticity, resulting in vessels which do not distend and contract and which have thickened walls and narrowed lumens. The end result is reduced blood flow or complete blockage. Examples of vascular diseases characterized by these pathophysiological processes include chronic progressive glomerular disease, e.g., diabetic-induced glomerulosclerosis (scarring); progressive renal failure after renal transplantation; occlusion of shunts used to provide vascular access in patents with endstage renal disease being treated with hemodialysis; other chronic small blood vessel diseases (such as in some patients with hypertension); recurrence of stenosis in patients who have undergone coronary bypass surgery; and diabetic retinopathy.

"Vascular disease treatments" include but are not limited to treatment of peripheral artery diseases (e.g. with cholesterol-lowering medications, high blood pressure medications, medication to control blood sugar, medications to prevent blood clots, symptom-relief medications, angioplasty and surgery, thrombolytic therapy and supervised exercise programs), cerebrovascular disorder treatments (e.g. aspirin, TPA, mechanical clot removal, carotid endarterectomy, angioplasty and stents), treatment of atherosclerosis (e.g. cholesterol medications, anti-platelet medications, beta blocker medications, angiotensin-converting enzyme (ACE) inhibitors, calcium channel blockers, water pills (diuretics), angioplasty, endarterectomy, thrombolytic therapy, and bypass surgery). These exemplified types and categories of treatments are illustrative, and those of ordinary skill in the art can readily

identified additional vascular diseases and treatments that can be assessed and treated in accordance with the methods of the invention.

These and other aspects of the invention are illustrated in the following non-limiting example.

Example 1

Summary of Experimental Results

Integrin $\alpha_v\beta_3$ is expressed on monocytes and may be used as target for imaging inflammation in vascular pathology.

Methods and Results: Expression of $\alpha_v\beta_3$ integrin was confirmed by flow cytometry in human monocytes and monocyte-derived macrophages. Integrin activation with $MnCl_2$ enhanced the binding of NC100692, a ^{99m}Tc labeled αv-specific tracer, to monocytes and macrophages. Vessel wall inflammation and remodeling was induced in murine carotid arteries through adventitial exposure to $CaCl_2$. *In vivo* NC100692 microSPECTCT imaging performed at 2 and 4 weeks after surgery demonstrated significantly higher tracer uptake in remodeling left, as compared to sham-operated right carotid arteries. Immuno-histological analysis at 4 weeks demonstrated significant expansive remodeling of left carotid arteries which contained a high number of macrophages. Macrophage infiltration in remodeling arteries was confirmed by real-time polymerase chain reaction. There was no significant difference in normalized α_v, β_3 or β_5 expression between right and left carotid arteries. Finally, *in vivo* NC100692 uptake strongly correlated with macrophage marker expression in carotid arteries.

Conclusions: NC100692 microSPECT imaging can detect vessel wall inflammation *in vivo* by targeting integrin activation. Thus, α_v-targeted imaging provides a novel non-invasive approach for identifying patients who are at high risk for vascular events and tracking the effect of anti-inflammatory treatments.

Example 1 demonstrates that peripheral blood monocytes and monocyte-derived macrophages express $\alpha_v\beta_3$ integrin, and bind to NC100692, a cyclic RGD peptide with specificity for activated α_v integrins [2, 5 6] to levels comparable to that of endothelial cells

(ECs). In a mouse model of vessel wall inflammation, NC100692 uptake was clearly detectable by microSPECT/CT imaging in chemically injured carotid arteries and the uptake correlated well with the presence of macrophages.

Material and Methods

Materials

Materials were obtained from Sigma (St. Louis, MO), unless indicated otherwise. NC100692 precursor and its fluorescent-labeled homologue were provided by GE healthcare (Buckinghamshire, UK). NC100692 radiolabeling with ^{99m}Tc was performed using kits provided by GE according to the manufacturer's instructions [6]. Each kit contains approximately 44 nmol NC100692 (molecular weight 1697) and was labeled with 1.1 GBq sodium pertechnetate (^{99m}Tc).

Cell Culture

Human umbilical vein endothelial cells were isolated and cultured as described [7]. Peripheral blood mononuclear cells (PBMCs) were isolated under protocols approved by the Yale Human Investigation Committee from normal anonymous donors' leukapheresis product by gradient density centrifugation following standard procedures. Monocytes were isolated to high purity from PBMCs by magnetic cell sorting using anti-CD14-coated beads according to manufacturer's instructions (Stemcell Technologies, Vancouver, BC). Monocyte purity was verified by flow cytometry and was found to be >85%. Purified monocytes were cultured for 10 days in RPMI plus 10% fetal bovine serum (Lonza, Walkersville, MD),2 mM L-glutamine, 100 U/ml penicillin and 100 ug/ml streptomycin in the presence of recombinant GM-CSF (50n9/ml, PeproTech, Rocky Hill, NJ) to generate type 1 macrophages 8.

Flow cytometry

Expression of surface proteins was analyzed by staining live cells with conjugated anti-CD3 (BD pharmigen, San Jose, CA), CD14 (BD pharmigen), $\alpha_v\beta_3$ integrin (LM609, Millipore corporation, Temecula,CA) antibody, the corresponding isotype control antibodies or a fluorescent RGD peptide homologue of NC100692 (GE Healthcare). To

investigate the effect of integrin activation, harvested cells were exposed to MnClz (0.2 mM) in calcium and magnesium free phosphate buffered saline for 10 minutes before staining. $MnCl_2$was kept in all buffers during staining and flow cytometry. At least 2,500 cells that satisfied a gate on forward and side scatter were acquired using a FACS Calibur flow cytometer (Becton Dickinson, Mountain View, CA). Data analysis was performed using CellQuest software (San Jose, CA).

Animal model

Twenty animals underwent surgery to induced carotid artery inflammation and remodeling as described e. Briefly, in 8- to 1O-week old female apoEr- mice (Jackson Laboratory, Bar Harbor, ME, n=96) fed a high-cholesterol chow (1.25% cholesterol, Harlan Teklad, Madison, WI) for 1 week the carotid arteries were surgically exposed under anesthesia (ketamine 100 mg/kg and xylazine 10 mg/kg, ip), The left common carotid artery just below carotid bifurcation was advetageously exposed to a 10% solution of $CaCl_2$ for 20 minutes. The opposite carotid artery was exposed to normal saline and served as control for imaging studies. Ibuprofen (0.11 mg/kglday, po) was used for postoperative analgesia. Experiments were performed according to regulations of Yale University's Animal Care and Use Committee.

Imaging

MicroSPECT/CT imaging was performed as described [9, 10] with minor modifications on 9 animals at two weeks after surgery. Of these, 5 underwent repeat imaging followed by tissue analysis at 4 weeks. Images could not be obtained from two of this latter group of animals. An additional group consisting of 5 animals underwent imaging followed by tissue analysis at 4 weeks. lmages obtained at either 2 (n=9)or 4 (n=8) weeks were combined for analysis of tracer uptake at each time point. Briefly, 41 ± 1.1 MBq NC100692 ^{99m}Tc-labeled) was administered through a right jugular vein intravenous catheter placed under anesthesia (isofluorane 1-3%). Animals were imaged after 2 hours on a high-resolution small animal imaging system (X-SPECT, Gamma Medicaldeas, Northridge, CA)with 1-mm low-energy pinhole collimators. The following acquisition parameters were used for microSPECT imaging: 360 degree, 128 projections, 30 seconds/projection (-80 minute image acquisition), with 140 keV

photopeaks ±10% window. After completion of microSPECT imaging, animals were injected with a continuous infusion of iodinated CT contrast (iohexol 100 µl/min) over 2 minutes or Fenestra (200 µl, ART Advanced Research Technologies, Montreal, QC, Canada), and CT imaging was performed (energy 75 kVp/280 µA, matrix 512x512)lo identify anatomic structure. To avoid tissue damage we did not perform any additional *ex vivo* imaging and preserved the tissue immediately for mRNA and immune histological analysis. To establish imaging specificity, three animals were injected with 5O-fold excess unlabeled precursor prior to NC100692 imaging at two weeks after surgery. For quantitative analysis of tracer uptake, cylindrical regions of interest (ROIs) were drawn at the level of carotid artery bifurcation (2x2x2 mm). A ROI immediately posterior to both carotids was used to calculate the background activity. Data were expressed as background-corrected counts per voxel (cpv)/MBq injected.

Morphometric analysis and immunostaining

After imaging, carotid arteries were harvested, embedded in OCT compound, snap-frozen, and stored at -80'C. Hematoxylin and eosin immunostaining were performed according to standard protocols on 5µm-thick cryostat sections. Morphometric analysis was performed on cryostat sections with NIH ImageJ software (National Institutes of Health, Bethesda, MD), as previously described [11]. The area within the external elastic lamina representing total vessel area was calculated by averaging measurements from serial sections at 200µ m intervals from 200 µm to 2,000 µm below carotid bifurcation. For immunostaining, primary antibodies were anti-mouse αv integrin (Millipore), antismooth muscle α-actin (Sigma), anti-CD31 (BD Pharmingen, San Jose, CA), and F4/80 (Invitrogen, Carlsbad, CA). Isotope-matched antibodies were used as controls. Nuclei were detected with DAPI.

Quantitative reverse transcription polymerase chain reaction (RT-PCR)

Tissue was available from 8 animals for analysis. Total RNA was isolated, reverse transcribed, and real time RT-PCR performed as described [9] using the following Taqman@ primer sets (Applied Biosystems, Foster City, CA). CD68 (Mm00839636_g1), EMRI (Mm00802529_m1), smooth muscle α-actin (Mm01546133-m1), CD31 (Mm00476702-m1) and α_v (Mm00434506-m1), B3 (Mm00443980-m1), β5

(Mn00439825-m1), GAPDH (Mm99999915_91). The results were normalized to Glyceraldehyde 3-phosphate dehyd rogenase (GAPDH).

Statistical analysis

Statistical analysis was performed using GraphPad Prism (La Jolla, CA). Data are presented as mean ± standard error (SE). Differences between two groups were tested using two-tailed paired or unpaired Student's t test, as appropriate. Association between any 2 variables was addressed using Pearson correlation. Significance was set at the 0.05 level.

Results

$\alpha_v\alpha_3$ expression and activation in monocytes and macrophages

Monocytes and lymphocytes constitute a major component of inflammatory cells in the vessel wall. We assessed $\alpha_v\beta_3$ expression on human peripheral blood monocytes, monocyte-derived macrophages as well as ECs by flow cytometry, While $\alpha_v\beta_3$ integrin could not be detected by flow cytometry on lymphocytes (not shown), monocytes expressed high levels of the integrin (Fig 1). NC100692 is a cyclic RGD peptide with specificity for α_v integrins [2, 5]. To further investigate NC100692 binding properties, we assessed the binding of a fluorescent homologue of NC100692 to ECs by flow cytometry. Low level of NC100692 homologue binding was detected in resting ECs. However, integrin activation with $MnCl_2$ (0.2 mM) considerably enhanced peptide binding to ECs (Supplemental Fig 1). Similarly, integrin activation with $MnCl_2$ enhanced RGD peptide binding to monocytes (Fig 1a) without changing cell membrane $\alpha_v\beta_3$ expression (not shown), indicating that similar to resting ECs 12, α_v integrins on resting monocytes are in a non-fully activated state. Double color staining of monocytes using an anti- $\alpha_v\beta_3$ antibody and the fluorescent RGD peptide indicated that they both stain the same cells (Fig 1b). Interestingly, there were considerable differences in the extent of integrin activation in monocytes from different donors. To address the effect of monocyte differentiation into macrophages on α_v expression and NC100692 binding purified monocytes were differentiated into type I macrophages. Macrophage differentiation was confirmed by their distinct morphology. Similar to resting monocytes, macrophages expressed high levels of $\alpha_v\beta_3$ integrin and bound to NC100692. $MnCl_2$

enhanced fluorescent NC100692 binding to macrophages (Fig 1a) without altering the integrin expression level. Due to the time required for macrophage differentiation, monocytes and macrophages from the same donor were stained on different days. The changes in integrin expression and RGD peptide binding observed in the course of monocyte to macrophage differentiation were not consistent and varied from experiment to experiment imaging α_v integrin activation in vessel wall inflammation

To investigate α_v-targeted imaging for detection of vessel wall inflammation *in vivo*, we used an established model of vascular inflammation. In this model, adventitial application of $CaCl_2$ to common carotid arteries of high fat fed $apoE^{-/-}$ mice triggers an inflammatory response that leads to aneurismal dilatation of the artery over a period of 4 weeks [9]. $ApoE^{-/-}$ mice underwent ^{99m}Tc-NC100692 microSPECT imaging at 2 or 4 weeks after surgery. NC100692 signal was readily visible on inflamed left, but not sham-operated right, carotid arteries identified by CT angiography at either time point after surgery (Fig 2). Quantitative analysis of NC100692 uptake from *in vivo* images showed significantly higher tracer uptake in the left, as compared to control right, carotid arteries (0.52 ±0.09 vs 0.07 ± 0.02 cpv/MBq injected, n= 9, $p<0.001$ at 2 weeks, and 0.42 ± 0.04 vs 0.13 t 0.02 cpv/MBq injected, n = 8, $p<0.001$ at 4 weeks, Fig 2b). As expected, considerable NC100692 uptake was also present in the surgical wound. Tracer uptake specificity in inflamed arteries was investigated in a group of animals at two weeks after surgery who were pretreated with 5O-fold excess non-labeled precursor prior to ^{99m}Tc-NC100692 administration. Left carotid uptake was significantly reduced following administration of excess unlabeled precursor (0.16 ±0.03 cpv/MBq, n=3 vs 0.52 ±0.09 cpv/MBq without blocking, n=9, p=0.004), establishing specificity of NC100692 uptake (Fig 3).

Ex vivo analysis of Integrin expression and inflammation

As expected, total vessel area at 4 weeks after surgery was approximately 2-fold higher in $CaCl_2$ treated left, compared to NaCl-treated right, carotid arteries (respectively, 0.192 ± 0.010 and 0.093 ± 0.007 mm^2, n=8, $p<0.0001$, Fig 4). Immunostaining with a macrophagespecific marker, F4/80, showed the presence of a large number of macrophages in the vessel wall in injured arteries (Fig 5). CD31 (EC) and smooth muscle α-actin (VSMC staining demonstrated the presence of small blood vessels in the vessel wall (Supplemental

Fig 2). α_v integrin immunostaining was detected in the intima and media of injured arteries, and its distribution resembled macrophage staining (Fig 5).
Macrophage content of the vessel wall was quantified by real time RT-PCR which showed significantly higher levels of GAPDH-normalized CD68 and EMRI mRNA expression in injured, as compared to sham-operated arteries (n=8, p=9.03 for CD68 and 0.003 for EMR1, Fig 6a). Interestingly, while there was no difference in CD31 mRNA expression between right and left carotid arteries, smooth muscle α-actin mRNA expression was significantly reduced in aneurismal arteries, indicating loss of VSMCs (n=8, p=0.045). There was no significant difference in GAPDH-normalized α_v, β_3, or β_5 expression between control right and aneurismal left carotid arteries (Fig 6b).

Biological correlate of NC100692 uptake in carotid arteries

A number of cells in the vessel wall, including ECs, VSMCs and monocyte-derived macrophages, express α_v integrins and may be bind to NC100692 *in vivo*. To investigate the biological correlates of NC100692 uptake in carotid arteries, the presence of specific cells was assessed by real time RT-PCR using cell-specific markers. NC100692 uptake significantly correlated with CD68 (r=0.67, p=0.02, Fig 7) expression, while there was no correlation between NC100692 uptake and GAPDH normalized CD31, or smooth muscle α-actin expression (not shown).

Discussion

Example 1 demonstrated a similar preferential binding to integrin active conformation for NC100692, a cyclic RGD peptide. In monocytes and macrophages Mn-induced integrin activation enhanced RGD peptide binding, indicating that similar to ECs, α_v integrins in resting monocytes and macrophages are not in a fully activated state.

Inflammation plays a key role in the pathogenesis of several vasculopathies, including atherosclerosis and aneurysm. In atherosclerosis, vessel wall inflammation has been linked to plaque vulnerability and imaging vessel wall inflammation may help identify patients at high risk for acute coronary syndromes and stroke [20]. Similarly, vessel wall inflammation is linked to aortic aneurysm expansion and rupture and detection of vessel wall inflammation in vivo may help stratify patients based on their risk of rupture [21]. A number of tracers,

predominantly those targeting endothelial adhesion molecules (vascular cell adhesion molecule-1[22]), cellular metabolism (with ^{18}F-fluorodeoxy glucose [23, 24]and protease activity (matrix metalloproteinases [9, 25-28], cathepsins [29, 30]) have been studied for their ability to track vessel wall inflammation *in vivo*. Recently, *ex vivo* studies have raised the possibility of $\alpha_v\beta_3$ targeted imaging of vessel wall inflammation. Using autoradiography, ^{18}F-Galacto-RGD was shown to localize in atherosclerotic lesions and RGD uptake correlated with the density of nuclei and ^{3}H fluorodeoxy glucose uptake [31]. Similarly, RGD-Cy5.5 localized in the arterial wall following carotid ligation in the mouse and the uptake was detectable by *ex vivo* near infrared fluorescence reflectance imaging [32]. Here, we demonstrated that NC100692 microSPECT/CT imaging can detect remodeling carotid arteries in a prototypic model of vascular inflammation in apoE$^{-/-}$mice *in vivo*. Blocking with excess unlabeled precursor confirmed the specificity of NC100692 signal. A similar protocol was used to image matrix metalloproteinase activation in vascular remodeling, where the approach to *in vivo* quantification of carotid signal was validated with ex vivo measures of tracer uptake[9, 10, 28] $\alpha_v\beta_3$ targeted paramagnetic nanoparticles have been used to image atherosclerotic plaque angiogenesis by magnetic resonance imaging [3]. Unlike these nanoparticles, smaller probes such as NC100692 are not confined to intravascular space and any $\alpha_v\beta_3$ integrin expressing vascular cell may be target for NC100692 binding *in vivo*. The intense autofluorescence of elastic laminae did not permit direct co-localization of fluorescent RGD peptide with specific vascular cells. However, $\alpha_v\beta_3$ expressing proliferating ECs associated with angiogenesis and inflammatory cells are both components of inflammatory response in the vessel wall. Cellular content and target expression in the vessel wall is often measured by immunostaining. Because immunostaining is at best a semi-quantitative technique and only a limited number of histological sections (5-7 μm) are evaluated, such data may not reliably relate to imaging data obtained from much larger segments (-2mm) of the artery. Because the small size of murine carotid arteries prohibits the use of a more quantitative approach (e.g., Western blotting) for protein measurement, we relied on mRNA analysis to quantify macrophage content and integrin expression in carotid arteries. Using this approach, we found a strong correlation between NC100692 uptake *in vivo* and GAPDH-normalized CD68 (macrophage marker) expression in the vessel wall, validating α_v-targeted imaging for detection of vessel wall inflammation *in vivo*. Importantly, despite the marked difference in NC100692 uptake, there was no significant difference in α_v, β_3, or β_5 integrin expression between control and

remodeling carotid arteries. This, in conjunction with the preferential binding of NC100692 to active conformation of integrins, may indicate that α_v integrins are in an active state in remodeling arteries.

In conclusion, we demonstrate that NC100692, a tracer with preferential binding to active conformation of α_v integrins, specifically localizes in inflamed carotid arteries of apoE$^{-/-}$ mice and provides a signal that is detectable by microSPECT/CT imaging *in vivo*. NC100692 uptake in the artery correlates well with macrophage content of the vessel wall, indicating that this RGD peptide may be used to image vascular inflammation *in vivo*. Further validation of our observations in other models of vessel wall inflammation may lead to the development of a novel imaging approach for identifying patients who are at high risk for vascular events and tracking the effect of anti-inflammatory treatments.

References

1. Meoli DF, Sadeghi MM, Krassilnikova S, Bourke BN, Giordano FJ, Dione DP, Su H, Edwards DS, Liu S, Harris TD, MadriJA, Zaret BL, Sinusas AJ. Noninvasive imaging of myocardial angiogenesis following experimental myocardial infarction. J Clin lnvest.2004; tt3:7684-1691.
2. Hua J, Dobrucki LW, Sadeghi MM, Zhang J, Bourke BN, Cavaliere P, Song J, Chow C, Jahanshad N, van Royen N, Buschmann l, MadriJA, Mendizabal M, Sinusas AJ. Noninvasive imaging of angiogenesis with a 99mTc-labeled peptide targeted at alphavbeta3 integrin after murine hind limb ischemia. Circulation. 2005; Ll7:3255-3260.
3. Winter PM, Morawski AM, Caruthers SD, Fuhrhop RW, Zhang H, Williams TA, Allen JS, Lacy EK, Robertson JD, Lanza GM, Wickline SA. Molecular imaging of angiogenesis ¡n early-stage atherosclerosis with alpha(v)beta3-integrin-targeted nanopart¡cles. Circuløtion. 2003;108:2270- 2274.
4, Sipkins DA, Cheresh DA, KazemiMR, Nevin LM, Bednarsk¡ MD, LiKC. Detection of tumor angiogenesis in vivo by alphaVbeta3-targeted magnetic resonance imaging. Nat Med. 1998; 4:623-626.
5. lndrevoll B, Kindberg GM, Solbakken M, Bjurgert E, Johansen JH, Karlsen H, Mendizabal M, Cuthbertson A. NC-100717: a versatile RGD peptide scaffold for angiogenesis imaging. Bioorg Med Chem Lett. 2006; 16:6190-6193.

6. Edwards D, Jones P, Haramis H, Battle M, Lear R, Barnett DJ, Edwards C, Crawford H, Black A, Godden V. 99mTc-NC100692-a tracer for imaging vitronectin receptors associated with angiogenesis: a preclinical investigation. Nucl Med Biol. 2008; 35 :365-375.

7, Zhang J, Krassilnikova S, Gharaei AA, Fassaei HR, Esmailzadeh L, Asadi A, Edwards DS, Harris TD, Azure M, Tellides G, Sinusas AJ, Zaret BL, Bender JR, Sadeghi MM. Alphavbeta3-targeted detection of arteriopathy in transplanted human coronary arteries: an autoradiographic study. Foseb J. 2005; 19:1857-1859.

8. Verreck FA, de Boer T, Langenberg DM, Hoeve MA, Kramer M, Vaisberg E, Kastelein R, Kolk A, de Waal-Malefyt R, OttenhoffTH. Human lL-23-producing type 1 macrophages promote but lL-L0- producing type 2 macrophages subvert immunity to (myco)bacteria. Proc Natl Acad Sci U S A. 2004; t9t:4560-4565.

9. Razavian M, Zhang J, Nie L, Tavakoli S, Razavian N, Dobrucki LW, Sinusas AJ, Edwards DS, Azure M, Sadeghi MM. Molecular imaging of matrix metalloproteinase activation to predict murine aneurysm expansion in vivo. J Nucl Med.2010;51:L107-71-15.

10. Tavakoli S, Razavian M, ZhangJ, Nie L, Marfatia R, Dobrucki LW, Sinusas AJ, Robinson S, Edwards DS, Sadeghi MM. Matrix metalloproteinase activation predicts amelioration of remodeling after dietary modification in injured arteries. Arterioscler Thromb Vasc Biol. 20tl;3L:L02-L09..

11. Sadeghi MM, Krassilnikova S, ZhangJ, Gharaei AA, Fassaei HR, Esmailzadeh L, Kooshkabadi A, Edwards S, Yalamanchili P, Harris TD, Sinusas N,Zaret BL, Bender JR. Detection of injury-induced vascular remodeling by targeting activated alphavbeta3 integrin in vivo. Circulation. 2Q04; L10:84-90.

12, Tzima E, del Pozo MA, Shattil SJ, Chien S, Schwartz MA. Activation of integrins in endothelial cells by fluid shear stress mediates Rho-dependent c¡oskeletal alignment. *Embo* J.2001; 2O:4639-4647.

13. Hynes RO. lntegrins: bidirectional, allosteric signaling machines. *Cell.* 2002; 110:673-687.

14. Pampori N, Hato T, Stupack DG, Aidoudi S, Cheresh DA, Nemerow GR, Shattis J. Mechanisms and consequences of affinity modulation of integrin alpha(V)beta(3) detected with a novel patch-engineered monovalent ligand . J Biol Chem. 1999 ; 27 4:21609-21616.

15. Huang S, Endo Rl, Nemerow GR. Upregulat¡on of integrins alpha v beta 3 and alpha v beta 5 on human monocytes and T lymphocyes facilitates adenovirus-mediated gene delivery. J Virol. 1995;69:2257-2263.

16. Hermann P, Armant M, Brown E, Rubio M, lshihara H, Ulrich D, Caspary RG, Lindberg FP,

Armitage R, Maliszewski Ç Delespesse G, Sarfati M. The vitronectin receptor and its associated CD47 molecule mediates proinflammatory cytokine synthesis in human monocytes by interaction with soluble CD23. J Cell Biol.1999; t44:767-775.

17. Cai W, Niu G, Chen X. Imaging of integrins as biomarkers for tumor angiogenesis. Curr Pharm Des. 2008; 14:2943 -2973..
18. Haubner R, Beer AJ, Wang H, Chen X. Positron emission tomography tracers for imaging angiogenesis. Eur J Nucl Med Mol Imaging.2010; 37 Suppl 1:S86-103.
19. Dijkgraaf I, Boerman OC. Molecular imaging of angiogenesis with SPECT. Eur J Nucl Med Mol Imaging. 2010; 37 Suppl 1:S104-113.
20. Finn AV, Nakano M, Narula J, Kolodgie FD, Virmani R. Concept of vulnerable/unstable plaque. Arterioscler Thromb Vasc Biol. 2010 ; 30 :7282-7292.
21. Nordon IM, Hinchliffe RJ, Loftus IM, Thompson MM. Pathophysiology and epidemiology of abdominal aortic aneurysms. Nat Rev Cardiol.2071.
22 Kaufmann BA, Sanders JM, Davis C, Xie A, Aldred P, Sarembock IJ, Lindner JR. Molecular imaging of inflammation in atherosclerosis with targeted ultrasound detection of vascular cell adhesion molecule-1. Circulation. 2007; 116:276-284.
23. Rudd JH, Warburton EA, Fryer TD, Jones HA, Clark JC, Antoun N, Johnstrom P, Davenport AP, Kirkpatrick PJ, Arch BN, Pickard JD, Weissberg PL. Imaging atherosclerotic plaque inflammation with [18F]-fluorodeoxyglucose positron emission tomography. Circulation.2002; 105:2708- 271I.
24. Reeps C, Essler M, PelisekJ, SeidlS, Eckstein HH, Krause BJ. Increased 18F-fluorodeoxyglucose uptake in abdominalaortic aneurysms in positron emission/computed tomography is associated with inflammation, aortic wall instability, and acute symptoms. J Vasc Surg.2008;48:477-423; discussion 424.
25. Deguchi JO, Aikawa M, Tung CH, Aikawa E, Kim DE, Ntziachristos V, Weissleder R, Libby P.Inflammation in atherosclerosis: visualizing matrix metalloproteinase action in macrophages in vivo Circulation, 2006; 114 :55 -62.
26. Fujimoto S, Hartung D, Ohshima S, Edwards DS, Zhou J, Yalamanchili P, Azure M, Fujimoto A,Isobe S, Matsumoto Y, Boersma H, Wong N, Yamazaki J, Narula N, Petrov A, Narula J. Molecular imaging of matrix metalloproteinase in atherosclerotic lesions: resolution with dietary modification and statin therapy. J Am Coll Cardiol.2008;52:1847-1857.
27. Lancelot E, Amirbekian V, Brigger I, Raynaud JS, Ballet S, David C, Rousseaux O, Le Greneur S, Port M, Lijnen HR, Bruneval P, Michel JB, Ouimet T, Roques B, Amirbekian S,

Hyafil F, Vucic E, Aguinaldo JG, Corot C, Fayad ZA. Evaluation of matrix metalloproteinases in atherosclerosis using a novel noninvasive imaging approach. Arterioscler Thromb Vasc Biol. 2008; 28 425-432.

28. Zhang J, Nie L, Razavian M, Ahmed M, Dobrucki LW, Asadi A, Edwards DS, Azure M, Sinusas AJ, Sadeghi MM. Molecular imaging of activated matrix metalloproteinases in vascular remodeling. Circulation. 2008; 118:1953-1960.
29. Nahrendorf M, Waterman P, Thurber G, Groves K, Rajopadhye M, Panizzi P, Marinelli B, Aikawa E, Pittet MJ, Swirski FK, Weissleder R. Hybrid in vivo FMT-CT imaging of protease activity in atherosclerosis with custom¡zed nanosensors. ArteriosclerThromb Vasc Biol, 2009; 29:1444-1451.
30. Kim DE, Kim JY, Schellingerhout D, Kim EJ, Kim HK, Lee S, Kim K, Kwon lÇ Shon SM, Jeong SW, Kim SH, Lee DK, Lee MM, Kim GE. Protease imaging of human atheromata captures molecular information of atherosclerosis, complement¡ng anatomic imaging. Arterioscler Thromb Vosc Biol. 2010; 30:449-456.
31. Laitinen l, Saraste A, Weidl E, Poethko T, Weber AW, Nekolla SG, Leppanen P, Yla-Herttuala S, Holzlwimmer G, Walch A, Esposito l, Wester HJ, KnuutiJ, Schwaiger M. Evaluation of alphavbeta 3 integrin-targeted positron emission tomography tracer 18F-galacto-RcD for imaging of vascular inflammation in atherosclerot¡c mice. Circ Cardiovasc lmaging.2009; 2, 333-338..
32, Waldeck J, Hager F, Holtke C, Lanckohr Ç von Wallbrunn A, Torsello G, Heindel W, Theilmeier G, Schafers M, Bremer C. Fluorescence reflectance imaging of macrophage-rich atherosclerotic plaques using an alpha beta 3 integrin-targeted fluorochrome. J Nucl Med. .2008; 49:1845-1851..

What is claimed is:

1. A method of assessing a vascular disease, and optionally, vascular remodeling in a subject, the method comprising:

(a) administering a detectable ligand having a binding affinity for an integrin to the subject, measuring the subject's vascular uptake of the detectable ligand, and comparing the subject's vascular uptake of the detectable ligand to a first standard or control, wherein an increase in the subject's vascular uptake of the detectable ligand when compared to the standard or control indicates that the subject suffers from, or is risk of developing, a vascular disease; and optionally

(b) imaging the subject's vascular walls to assess vascular wall inflammation or remodeling, wherein the presence of vascular wall remodeling when compared to a second standard or control indicates that the subject suffers from, or is at risk of developing, a vascular disease or its complications.

2. The method of claim 1, wherein the measurement of the subject's vascular uptake of the detectable ligand and optional imaging of the subject's vascular walls to assess vascular wall remodeling is conducted using an imaging technique selected from the group consisting of single photon emission tomography (SPECT), positron emission tomography (PET), near-infrared (NIR) fluorescence detection, magnetic resonance imaging (MRI), ultrasound, optical imaging and/or optoacoustic imaging.

3. The method of claim 1 or 2 wherein said integrin is $\alpha_v\beta_3$ integrin.

4. The method of claim 3, wherein the detectable ligand having a binding affinity for $\alpha_v\beta_3$ integrin is selected from the group consisting of labeled NC100692, a detectable $\alpha_v\beta_3$ integrin antibody, Vitaxin, Vitaxin-2–conjugated, gadolinium-encapsulated and a labeled $\alpha_v\beta_3$ integrin binding peptide.

5. The method of claim 3 wherein said detectable ligand is selected from the group consisting of a radiolabeled RGD peptide selected from the group consisting of ^{99m}Tc-NC100692, ^{18}F-AH111585, ^{111}In-RP748 , ^{18}F-galacto-RGD and ^{99m}Tc-3PRGD2.

6. The method of claim 3 wherein said detectable ligand is selected from the group consisting of ^{99m}Tc-NC100692 and ^{18}F-AH111585.

7. The method of claim 3 wherein said detectable ligand is selected from the group consisting of ^{99m}Tc-NC100692.

8. The method of claim 3 wherein said labeled detectable ligand is a RGD peptide labeled with a SPECT, PET or NIR reporter.

9. The method of claim 1, wherein the detectable ligand having a binding affinity for $\alpha_v\beta_3$ integrin is comprised of an $\alpha_v\beta_3$ integrin antibody, peptide, or peptide mimetic derivatized with or linked to a detectable moiety selected from the group consisting of: (a) a fluorescent label; (b) the bio-luminescent labels luciferase and luciferin; (c) a sensitizer; (d) a coenzyme or enzyme substrate; (e) a radiolabel; (g) labelled avidin or streptavidin; (h) a latex or carbon particle; and (i) biotin, digoxygenin or 5-bromodeoxyuridine.

10. The method of claim 9, wherein the detectable moiety is selected from the group consisting of:
(a) fluorescein and its derivatives, fluorochrome, GFP (Green Fluorescent Protein), dansyl, umbelliferone, phycoerythrin, phycocyanin, allophycocyanin, o-phthaldehyde, fluorescamine; a fluorophore lanthanide cryptates, a chelate, a chemoluminescent label, the chemiluminescers isoluminol and luminol and a dioxetane;

(b) luciferase and luciferin;

(c) a sensitizer;

(d) alkaline phosphatase, glucose-6-phosphate dehydrogenase (G6PDH), alpha-D-galactosidase, glucose oxydase, glucose amylase, carbonic anhydrase, acetylcholinesterase, lysozyme, malate dehydrogenase, lysozyme, peroxidase, and horseradish peroxidase;

(e) ^{18}fluorine, ^{64}copper, ^{65}copper, ^{11}carbon, ^{67}gallium, ^{68}gallium, ^{77}bromine, ^{80m}bromine, ^{123}iodine, ^{124}iodine, ^{125}iodine, ^{126}iodine, ^{133}iodine, ^{111}Indium, and nitride or oxide forms derived thereof;

(f) a radiolabel selected from the group consisting of the alpha emitters ^{213}bismuth, ^{213}lead and ^{225}actinium; and

(g) labelled avidin or streptavidin.

11. The method of claim 1, wherein the method comprises the steps of:
(a) administering a detectable ligand having a binding affinity for $\alpha_v\beta_3$ integrin to the subject, said detectable ligand having a binding affinity for $\alpha_v\beta_3$ integrin being selected from the group consisting of ^{111}In-MSAP-RGD, (18)F-galacto-RGD ((18)F-RGD, (18)F-AlF-NOTA-PRGD2, [(99m)Tc]HYNIC-RGD [6-hydrazinonicotinic acid conjugated to cyclo(Arg-Gly-Asp-D-Phe-Lys), (99m)Tc-RAFT-RAD, (64)Cu-RGD, 18F-FBEM, and [18F]fluciclatide;

(b) measuring the subject's vascular uptake of the detectable ligand having a binding affinity for $\alpha_v\beta_3$ integrin using an imaging technique selected from the group consisting of PET and SPECT; and optionally

(c) imaging the subject's vascular walls to assess vascular wall remodeling using Positron Emission Tomography (PET) and Single Photon Emission Computed Tomography (SPECT).

12. The method of claim 1, wherein the method comprises the step of measuring the subject's vascular uptake of the detectable ligand having a binding affinity for $\alpha_v\beta_3$ integrin using positron emission tomography (PET), single photon emission computed tomography (SPECT), computed tomography (CT), optoacoustic imaging, and magnetic resonance imaging (MRI).

13. The method of claim 1, wherein the detectable ligand having a binding affinity for $\alpha_v\beta_3$ integrin is selected from the group consisting of an $\alpha_v\beta_3$ integrin antibody, a peptide, and a peptide mimetic, wherein each of said $\alpha_v\beta_3$ integrin antibody, a peptide, and peptide mimetic is conjugated to the detectable moiety by a linker.

14. The method of claim 13, wherein the linker is selected from the group consisting of diethylenetriamine pentaacetate (DTPA)-isothiocyanate, succinimidyl 6-hydrazinium nicotinate hydrochloride (SHNH), and hexamethylpropylene amine oxime (HMPAO).

15, The method of claim 14, wherein derivatization of the detectable ligand is enhanced by a chelator.

16. The method of claim 1 wherein the vascular disease is an aneurysm, atherosclerosis, acute coronary syndrome, stroke, vasculitis or transplant vasculopathy.

17. The method of claim 1 wherein said assessing tracks the effectiveness of therapeutic intervention on at least one vascular disease.

18. The method of claim 17 wherein said vascular disease is ischemic stroke, hemorrhagic stroke, transient ischemic attack (TIA), vascular inflammation due to meningitis, atherosclerosis, thrombi or emboli resulting from atherosclerosis, arteritis, physical obstruction of arterial blood supply to the brain, lacunar stroke, hypoperfusion emboding diffuse injury caused by non-localized cerebral ischemia, myocardial infarction and arrhythmia, restenosis associated with percutaneous transluminal coronary angioplasty, peripheral vascular disease and cerebral vascular disease, venous occlusive disorders such as deep vein thrombosis, hypercoagulopathies, aneurysms and chronic progressive vascular disease.

19. The method according to claim 17 wherein said vascular disease is aortic aneurysm, atherosclerosis, acute coronary syndrome, stroke, vasculitis and transplant vasculopathy.

20. The method of claim 1, wherein the method comprises the steps of:
(a) administering a detectable ligand having a binding affinity for $\alpha_v\beta_3$ integrin selected from the group consisting of an $\alpha_v\beta_3$ integrin antibody, peptide, and peptide mimetic to the carotid artery of the subject;

(b) imaging the subject's carotid artery at about 2 to about 4 hours after administration of the detectable ligand using microSPECT;

(c) thereafter measuring detectable ligand uptake by the carotid artery; and optionally

(d) excising a tissue sample from the carotid artery and determining carotid artery vascular remodeling by imaging the tissue sample.

21. The method of any of claims 1-15, wherein the vascular disorder is selected from the group consisting of ischemic stroke, hemorrhagic stroke, transient ischemic attack (TIA), vascular inflammation due to meningitis, atherosclerosis, acute coronary syndrome, stroke, thrombi or emboli resulting from atherosclerosis, arteritis, physical obstruction of arterial blood supply to the brain, lacunar stroke, hypoperfusion emboding diffuse injury caused by non-localized cerebral ischemia, myocardial infarction and arrhythmia, restenosis associated with percutaneous transluminal coronary angioplasty, peripheral vascular disease and cerebral vascular disease, venous occlusive disorders, deep vein thrombosis, hypercoagulopathies, aneurysms, vasculitis, and chronic progressive vascular disease (CPVD).

22. A method of assessing the efficacy of a vascular disease treatment and/or predicting vascular modeling in response to said treatment which has been administered to a subject who has been diagnosed as suffering from a vascular disease, the method comprising:
(a) administering a detectable ligand having a binding affinity for $\alpha_v\beta_3$ integrin to the subject, measuring the subject's vascular uptake of the detectable ligand, and comparing the subject's vascular uptake of the detectable ligand to a first standard or control, wherein a decrease in the subject's vascular uptake of the detectable ligand when compared to the standard or control indicates that the treatment is effective in treating the vascular disease; and optionally

(b) imaging the subject's vascular walls to assess vascular wall remodeling and optionally predict further vascular wall remodeling, wherein a decrease in or absence of vascular wall remodeling when compared to a second standard or control indicates that the treatment is effective in treating the vascular disease.

23. The method of claim 22, wherein the measurement of the subject's vascular uptake of the detectable ligand and optional imaging of the subject's vascular walls to assess vascular wall remodeling is conducted using an imaging technique selected from the group consisting of single photon emission tomography (SPECT), positron emission tomography (PET), and near-infrared (NIR) fluorescence detection.

24. The method of claim 22, wherein the detectable ligand having a binding affinity for $\alpha_v\beta_3$ integrin is a labeled NC100692, a detectable $\alpha_v\beta_3$ integrin antibody, Vitaxin, Vitaxin-2–conjugated, gadolinium-encapsulated and a labeled $\alpha_v\beta_3$ integrin binding peptide.

25. The method of claim 22 wherein said detectable ligand is selected from the group consisting of a radiolabeled RGD peptide selected from the group consisting of ^{99m}Tc-NC100692, ^{18}F-AH111585, ^{111}In-RP748 , ^{18}F-galacto-RGD and ^{99m}Tc-3PRGD2.

26. The method of claim 23, wherein the detectable ligand having a binding affinity for $\alpha_v\beta_3$ integrin is comprised of an $\alpha_v\beta_3$ integrin antibody, peptide, or peptide mimetic derivatized with or linked to a detectable moiety selected from the group consisting of: (a) a fluorescent label; (b) the bio-luminescent labels luciferase and luciferin; (c) a sensitizer; (d) a coenzyme or enzyme substrate; (e) a radiolabel; (g) labelled avidin or streptavidin; (h) a latex or carbon particle; and (i) biotin, digoxygenin or 5-bromodeoxyuridine.

27. The method of claim 22, wherein the detectable moiety is selected from the group consisting of:

(a) fluorescein and its derivatives, fluorochrome, GFP (Green Fluorescent Protein), dansyl, umbelliferone, phycoerythrin, phycocyanin, allophycocyanin, o-phthaldehyde, fluorescamine; a fluorophore lanthanide cryptates, a chelate, a chemoluminescent label, the chemiluminescers isoluminol and luminol and a dioxetane;

(b) luciferase and luciferin;

(c) a sensitizer;

(d) alkaline phosphatase, glucose-6-phosphate dehydrogenase (G6PDH), alpha-D-galactosidase, glucose oxydase, glucose amylase, carbonic anhydrase, acetylcholinesterase, lysozyme, malate dehydrogenase, lysozyme, peroxidase, and horseradish peroxidase;

(e) ^{18}fluorine, ^{64}copper, ^{65}copper, ^{14}carbon, ^{67}gallium, ^{68}gallium, ^{77}bromine, ^{80m}bromine, ^{123}iodine, ^{124}iodine, ^{125}iodine, ^{126}iodine, ^{133}iodine, ^{111}Indium, and nitride or oxide forms derived thereof;;

(f) a radiolabel selected from the group consisting of the alpha emitters ^{213}bismuth, ^{213}lead and ^{225}actinium; and

(g) labelled avidin or streptavidin.

28. The method of claim 22, wherein the method comprises the steps of:
(a) arterially administering a detectable ligand having a binding affinity for $\alpha_v\beta_3$ integrin to the subject, said detectable ligand having a binding affinity for $\alpha_v\beta_3$ integrin being selected from the group consisting of ^{111}In-MSAP-RGD, (18)F-galacto-RGD ((18)F-RGD, (18)F-AlF-NOTA-PRGD2, [(99m)Tc]HYNIC-RGD [6-hydrazinonicotinic acid conjugated to cyclo(Arg-Gly-Asp-D-Phe-Lys), (99m)Tc-RAFT-RAD, (64)Cu-RGD, (18)F-galacto-RGD, (99m)Tc-RAFT-RAD, and 18F-FBEM, and [18F]fluciclatide;

(b) measuring the subject's vascular uptake of the detectable ligand having a binding affinity for $\alpha_v\beta_3$ integrin using an imaging technique selected from the group consisting of PET and SPECT; and optionally

(c) imaging the subject's vascular walls to assess vascular wall remodeling using Positron Emission Tomography (PET) and Single Photon Emission Computed Tomography (SPECT).

29. The method of claim 22, wherein the method comprises the step of measuring the subject's vascular uptake of the detectable ligand having a binding affinity for $\alpha_v\beta_3$ integrin using positron emission tomography (PET), single photon emission computed tomography (SPECT), computed tomography (CT), optical imaging, optoacoustic imaging, and magnetic resonance imaging (MRI).

30. The method of claim 22, wherein the detectable ligand having a binding affinity for $\alpha_v\beta_3$ integrin is selected from the group consisting of an $\alpha_v\beta_3$ integrin antibody, a peptide, and a peptide mimetic, wherein each of said $\alpha_v\beta_3$ integrin antibody, a peptide, and peptide mimetic is derivatized with the detectable moiety by a linker.

31. The method of claim 30, wherein the linker is selected from the group consisting of diethylenetriamine pentaacetate (DTPA)-isothiocyanate, succinimidyl 6-hydrazinium nicotinate hydrochloride (SHNH), and hexamethylpropylene amine oxime (HMPAO).

32. The method of claim 31, wherein derivatization of the detectable ligand is enhanced by a chelator.

33. The method of claim 22, wherein the method comprises the steps of:
(a) administering a detectable ligand having a binding affinity for $\alpha_v\beta_3$ integrin selected from the group consisting of an $\alpha_v\beta_3$ integrin antibody, peptide, and peptide mimetic to the carotid artery of the subject;

(b) imaging the subject's carotid artery at about 2 to about 4 hours after administration of the detectable ligand using microSPECT;

(c) thereafter measuring detectable ligand uptake by the carotid artery; and optionally

(d) excising a tissue sample from the carotid artery and determining carotid artery vascular remodeling by imaging the tissue sample.

34. The method of claims 22-32, wherein the vascular disorder is selected from the group consisting of ischemic stroke, hemorrhagic stroke, transient ischemic attack (TIA), vascular inflammation due to meningitis, atherosclerosis, thrombi or emboli resulting from atherosclerosis, arteritis, physical obstruction of arterial blood supply to the brain, lacunar stroke, hypoperfusion emboding diffuse injury caused by non-localized cerebral ischemia, myocardial infarction and arrhythmia, restenosis associated with percutaneous transluminal coronary angioplasty, peripheral vascular disease and cerebral vascular disease, venous occlusive disorders, deep vein thrombosis, hypercoagulopathies and aneurysms.

FIGURE 1A

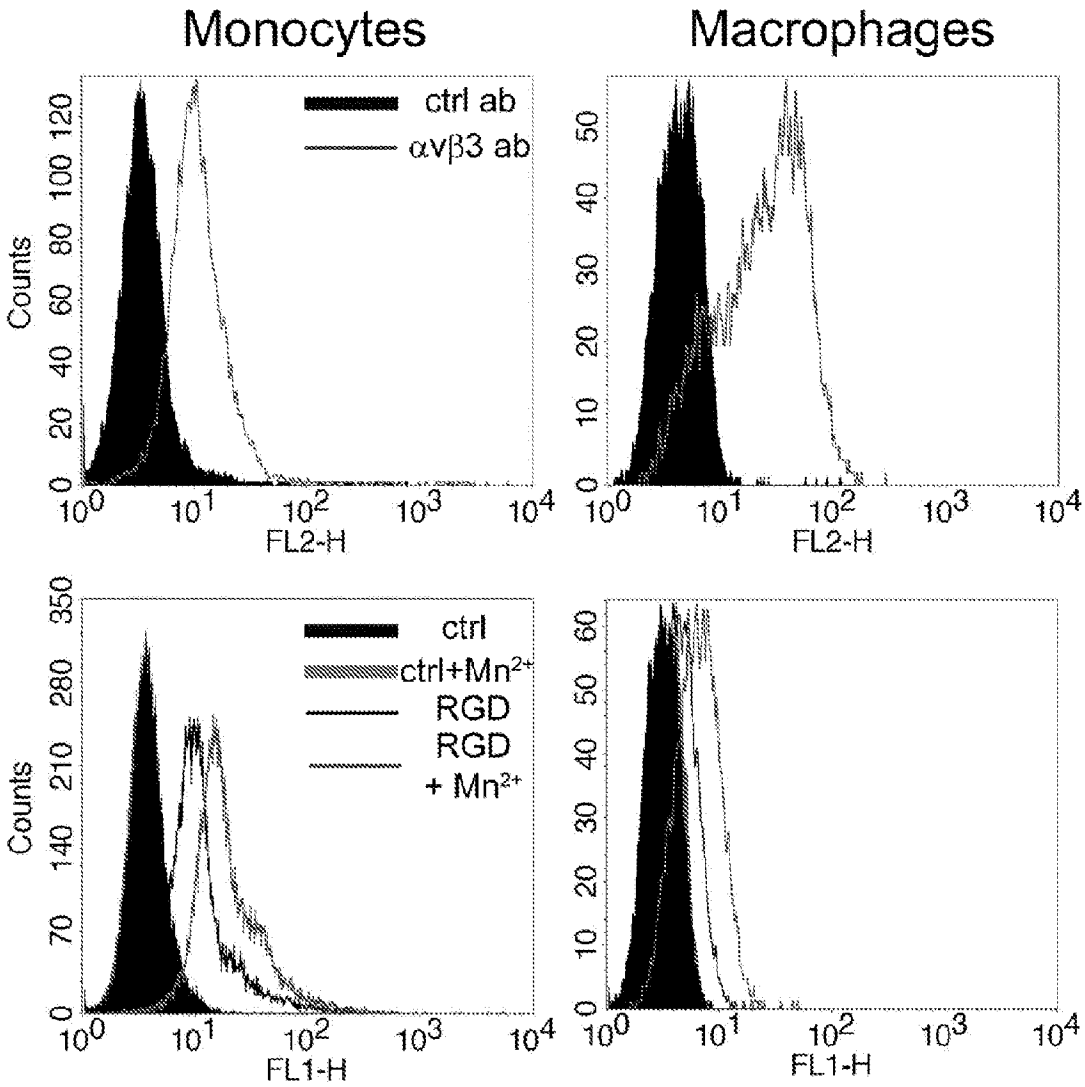
Monocytes
Macrophages
ctrl ab
αvβ3 ab
Counts
FL2-H
ctrl
ctrl+Mn2+
RGD
RGD
+ Mn2+
FL1-H

FIGURE 1B

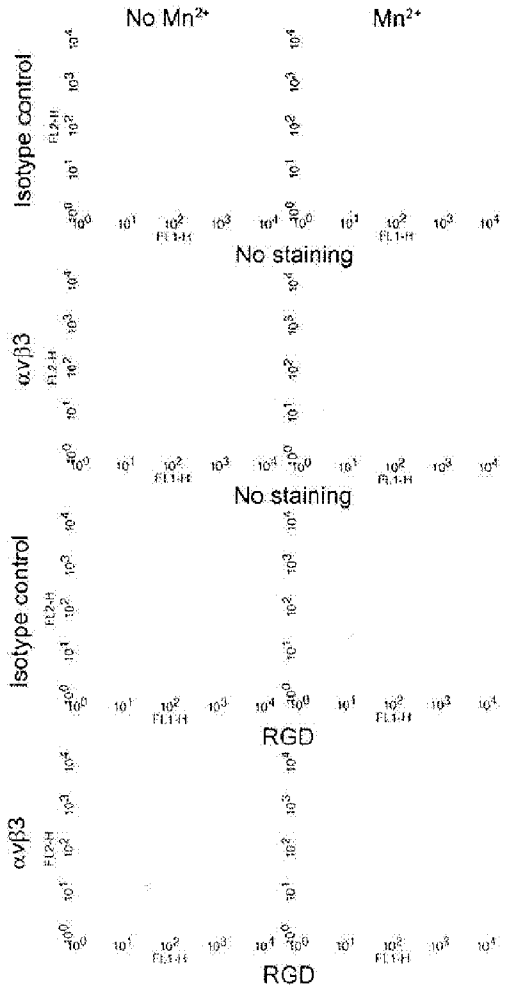
No Mn2+
Mn2+
Isotype control
No staining
αvβ3
No staining
Isotype control
RGD
αvβ3
RGD
FL2-H
FL1-H

FIGURE 2A

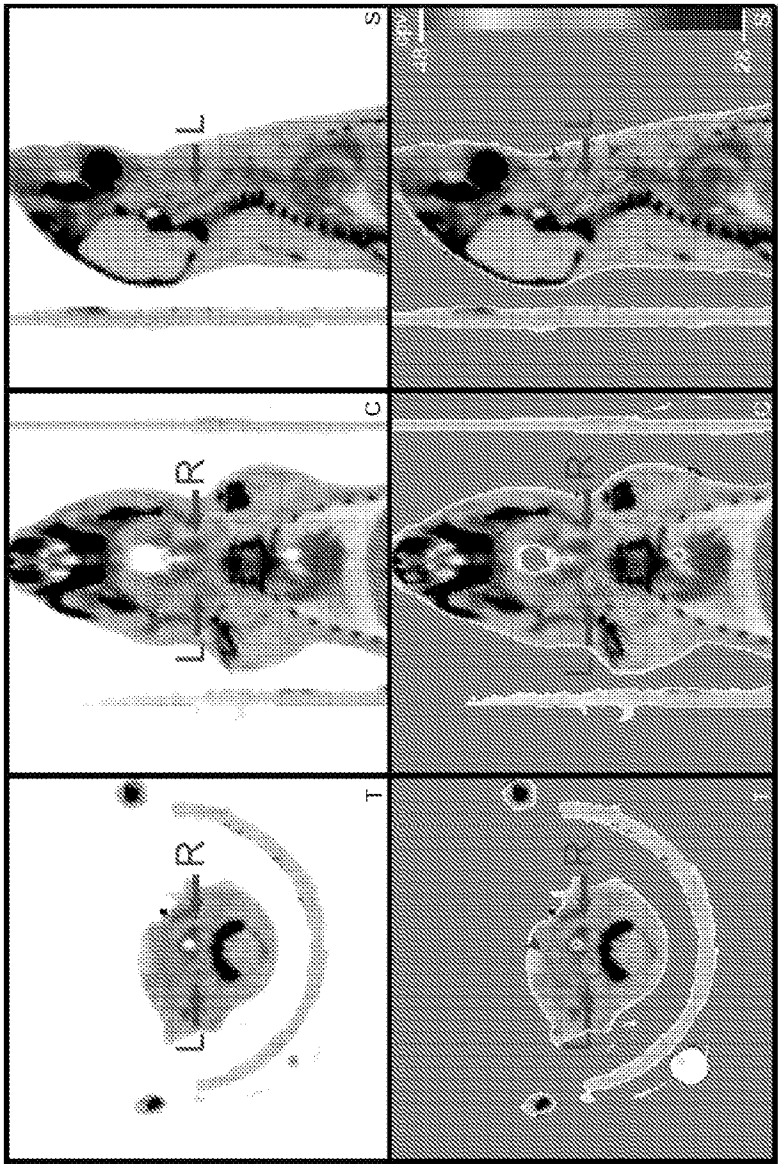

FIGURE 2B

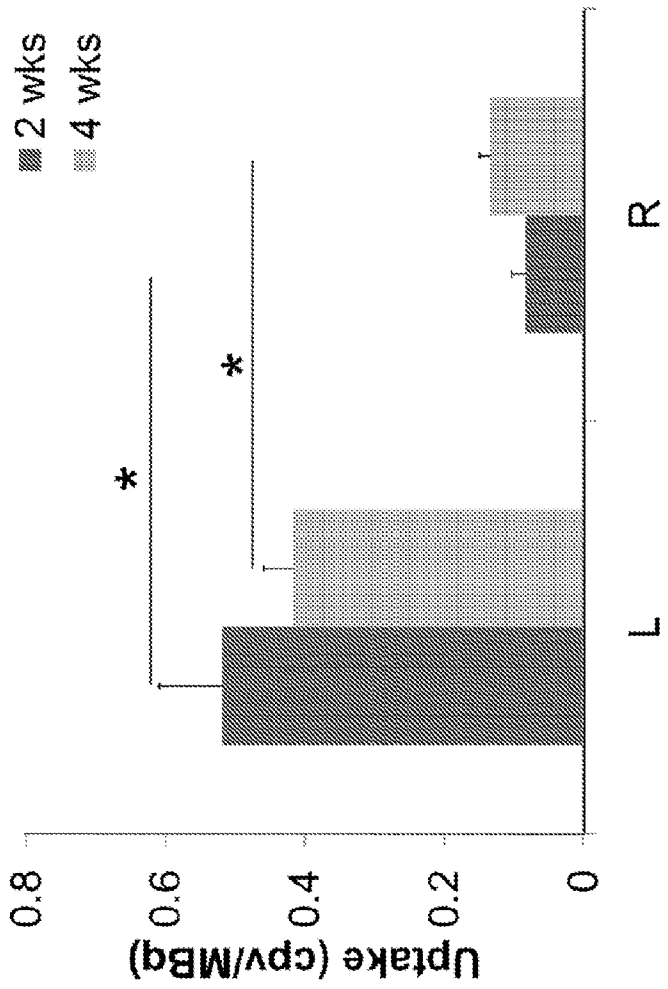

FIGURE 3

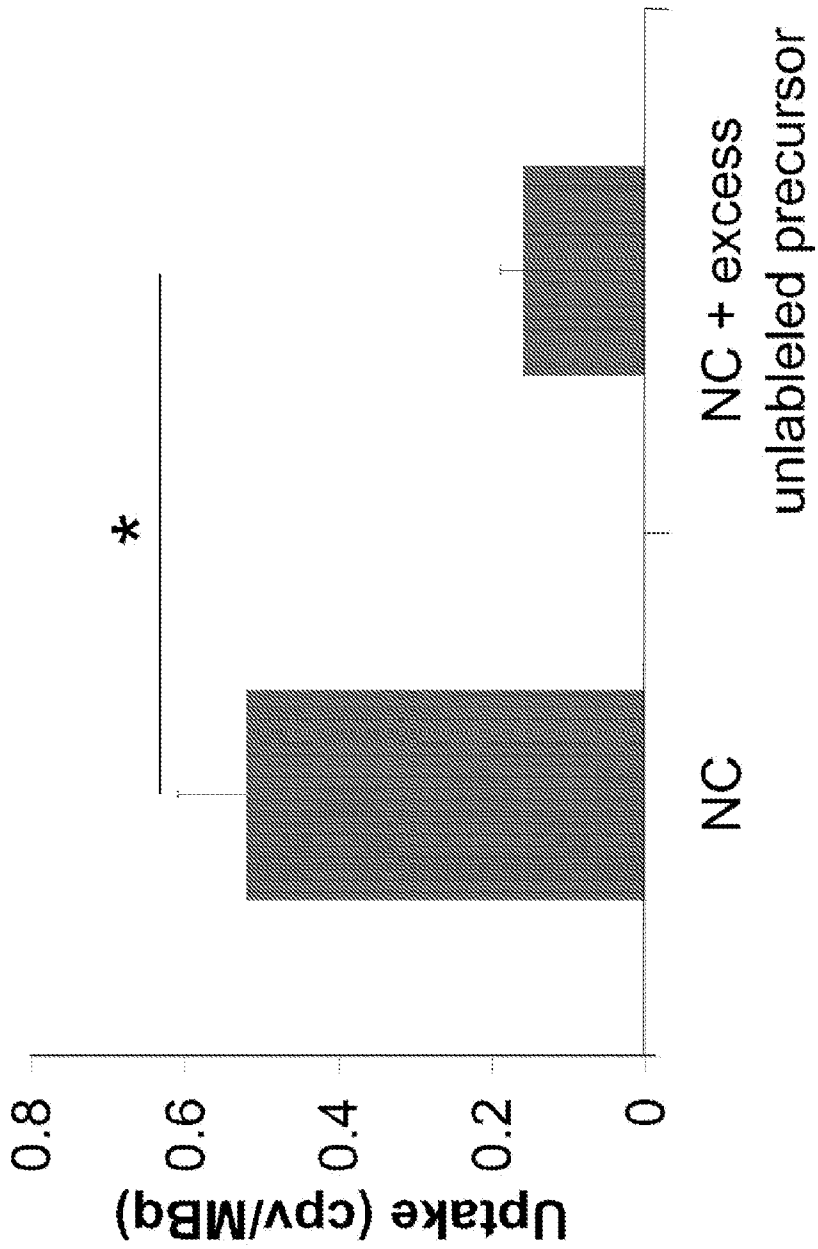
Uptake (cpv/MBq)
0.8
0.6
0.4
0.2
0
*
NC
NC + excess unlableled precursor

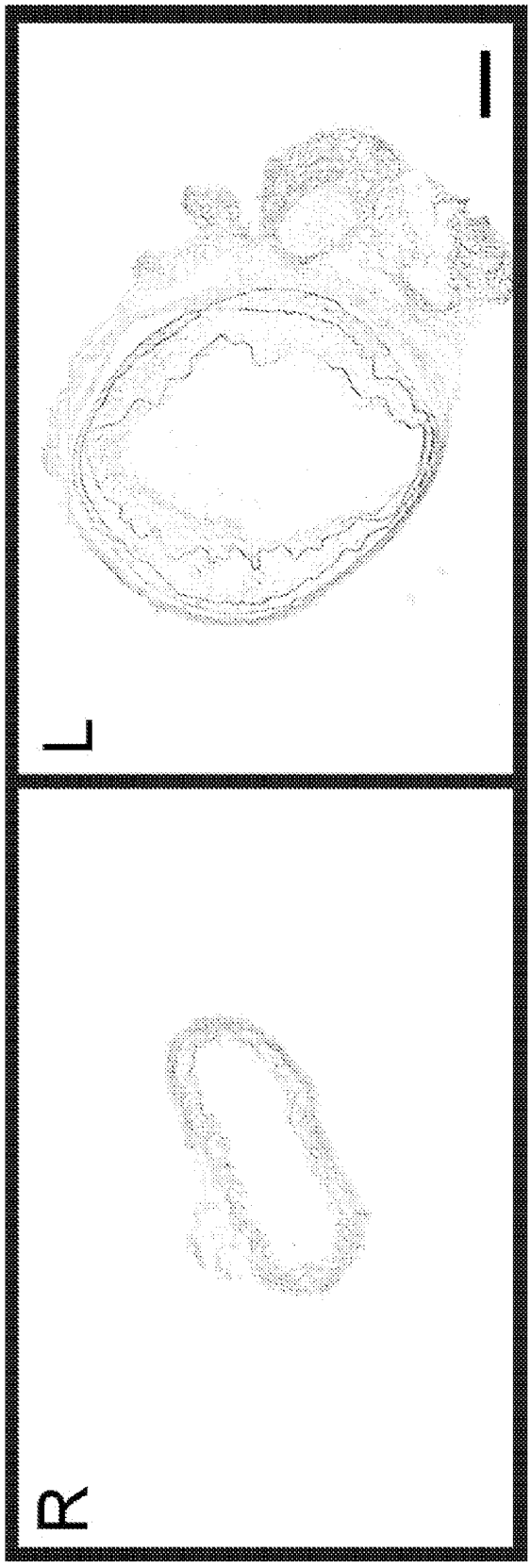

FIGURE 4A

FIGURE 4B

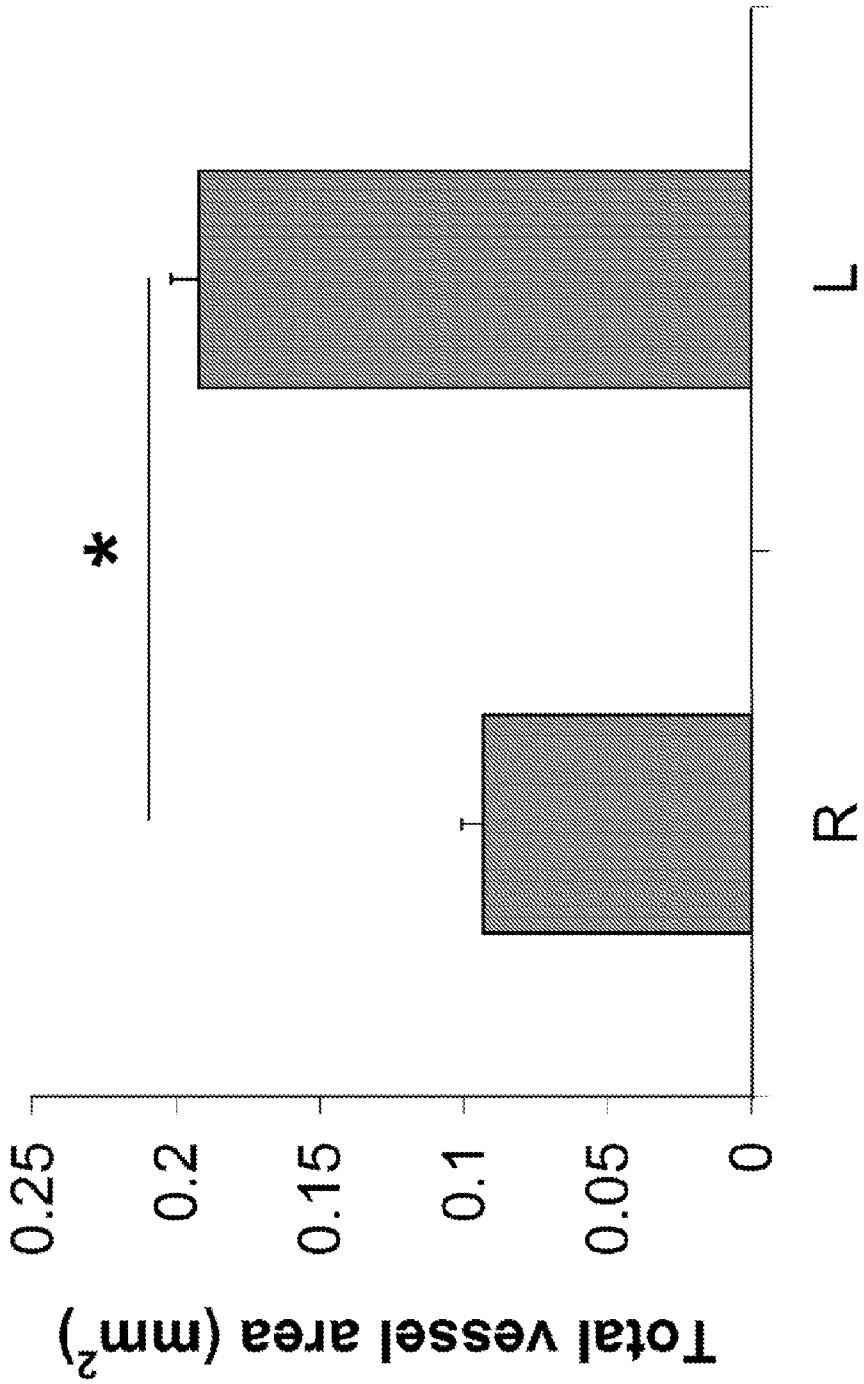

FIGURE 5

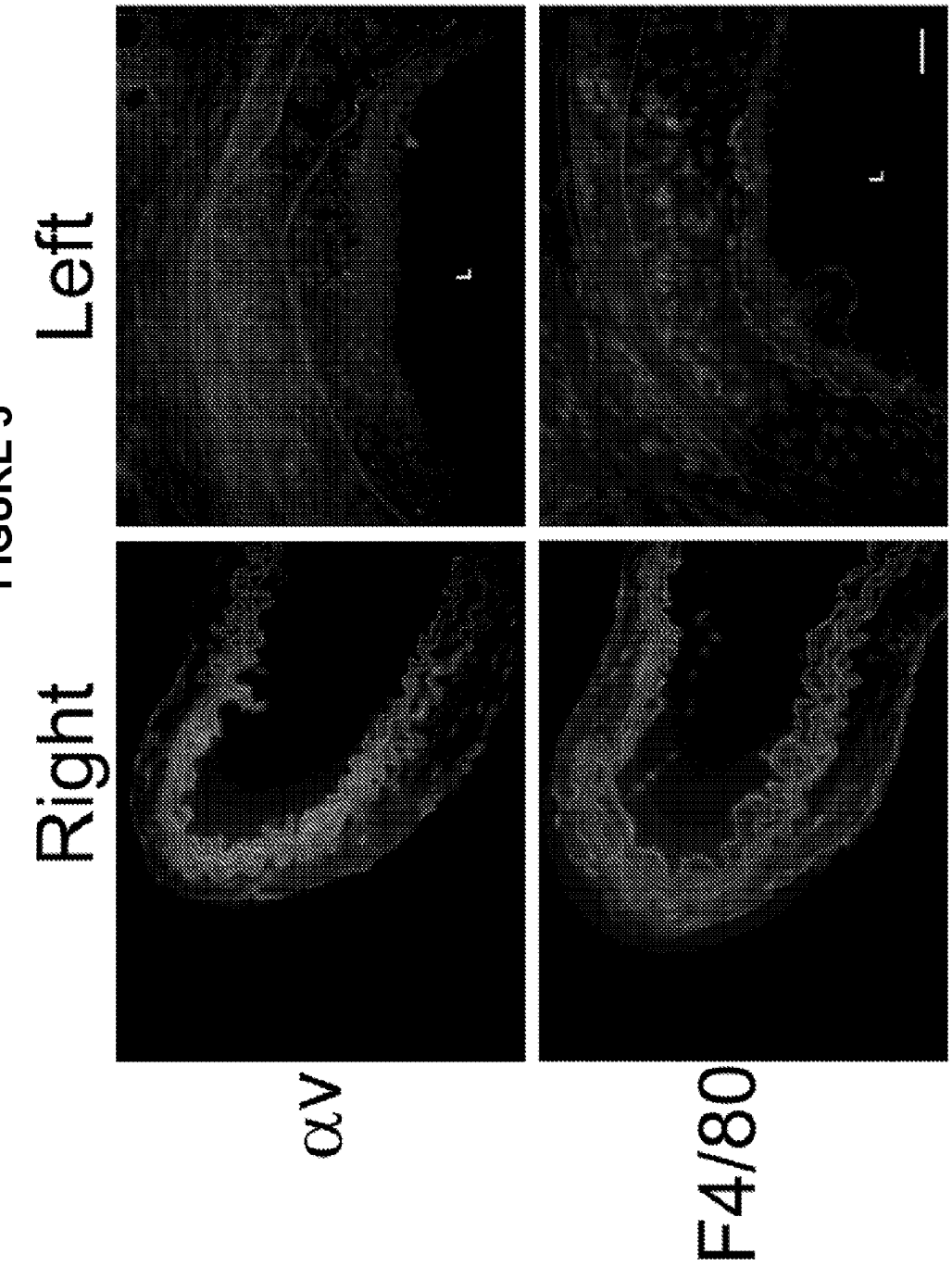

FIGURE 6A

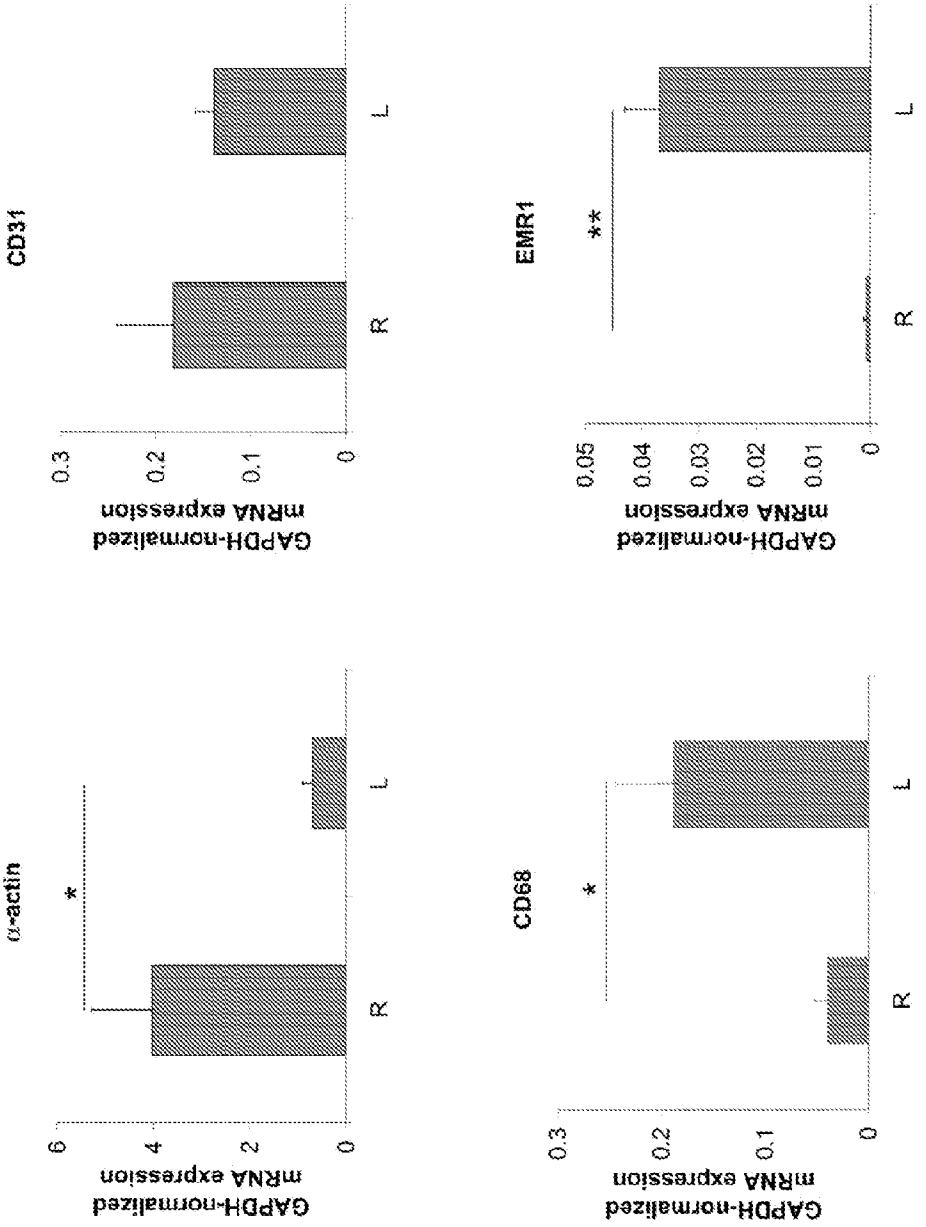
CD31
GAPDH-normalized mRNA expression
0
0.1
0.2
0.3
R
L
EMR1
**
GAPDH-normalized mRNA expression
0
0.01
0.02
0.03
0.04
0.05
R
L
α-actin
*
GAPDH-normalized mRNA expression
0
2
4
6
R
L
CD68
*
GAPDH-normalized mRNA expression
0
0.1
0.2
0.3
R
L

FIGURE 6B

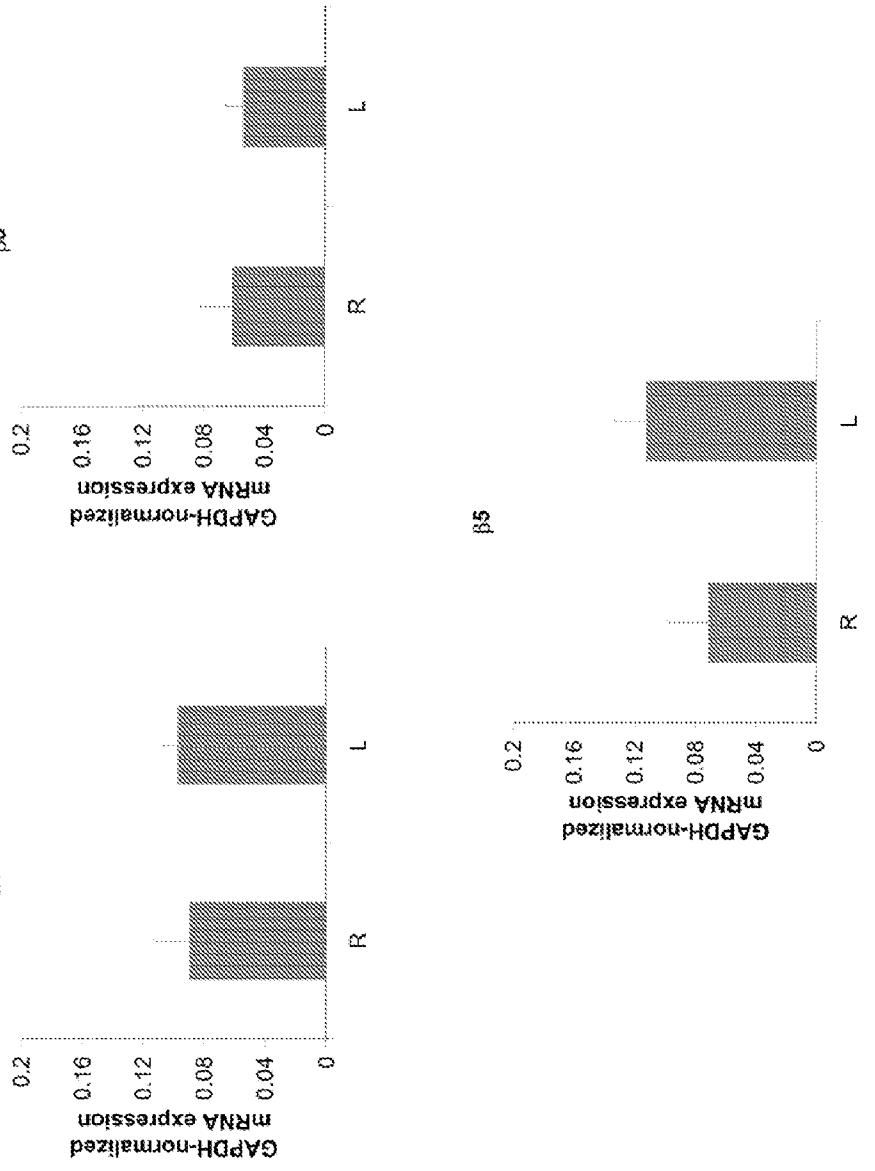
αV
β3
β5
GAPDH-normalized mRNA expression
0.2
0.16
0.12
0.08
0.04
0
R
L

FIGURE 7

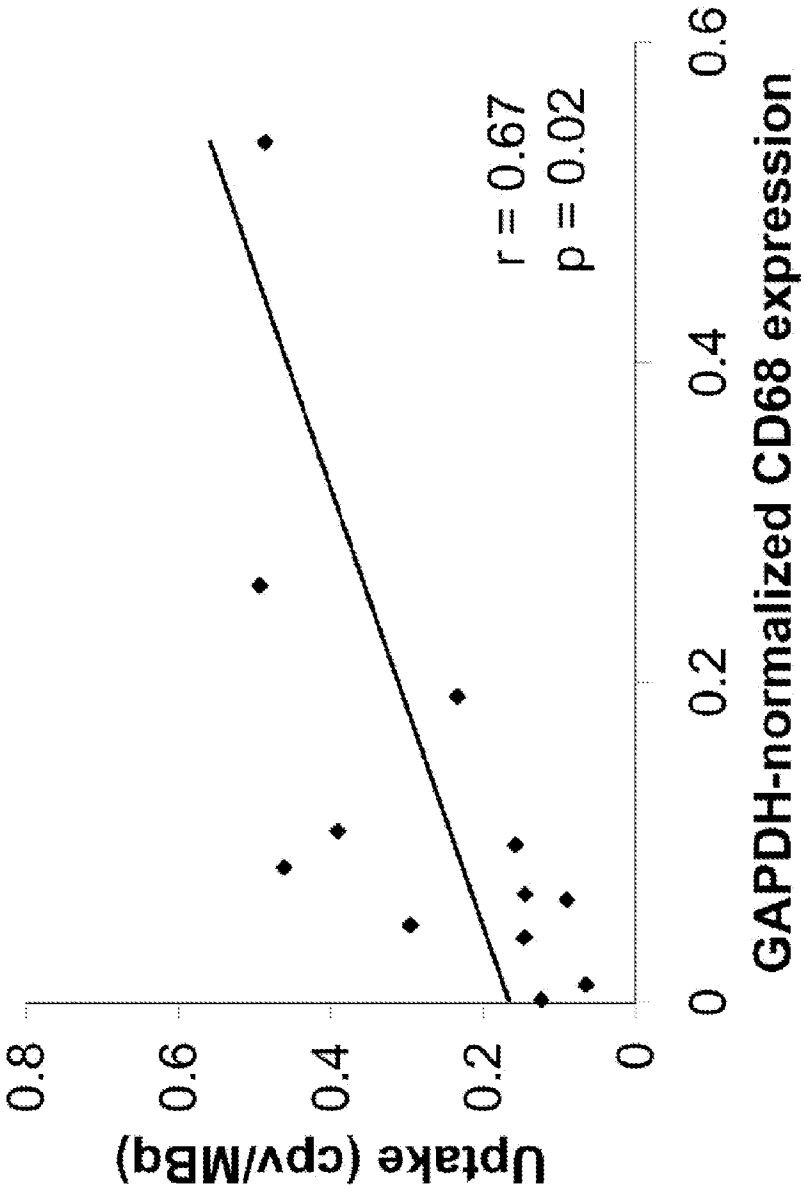
Uptake (cpv/MBq)
0.8
0.6
0.4
0.2
0
0
0.2
0.4
0.6
GAPDH-normalized CD68 expression
r = 0.67
p = 0.02

SUPPLEMENTAL FIGURE 1

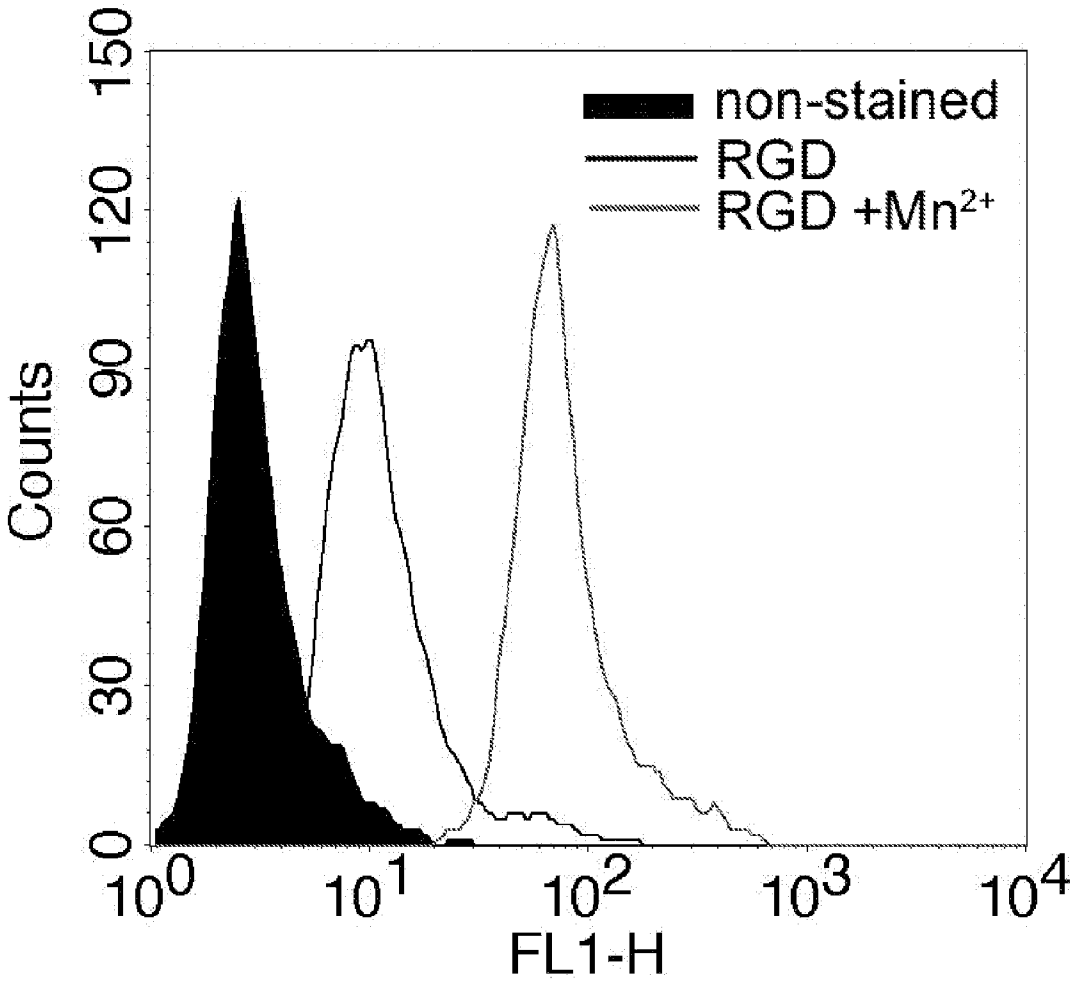

SUPPLEMENTAL FIGURE 2